

ORIGINAL RESEARCH ARTICLE

Influence of contemporary warming on landscape-zonal systems of the East-European sub-continent: Predictive empirical-statistical modeling

Erland G. Kolomyts

Pushchino Science Center of Russian Academy of Sciences, Institute of Basic Biological Problems, Institutskaya str., 1, Pushchino 129290, Russia. E-mail: egk2000@mail.ru

ABSTRACT

Presented in the given article regional geo-ecological prognoses are based on the construction of discrete empirical-statistical models of zonal and regional ecosystems. The analysis was carried out on the examples of the flat territories of the Volga River basin, as well as the northern macro-slope of the Main Caucasian ridge. Regional landscape-ecological calculations and mapping were carried out according to the global climatic models GISS-1988 and E GISS-2007 belonging to the family of models of general atmospheric circulation. The strategy of geo-ecological prognosis was as follows: first to identify the selected ecosystem objects (either zonal type of plant formations and regional kinds of landscape) to certain values of contemporary climatic conditions and then to estimate the most probable transformation of the revealed ecological niches of the given objects according to the expected climatic changes for the given prognostic date. The geo-ecological analysis has been performed using mainly two types of empirical models: (a) informational, describing the geo-component interrelations, serving as a basis for the regional bank of their ecological niches that characterizes their parametric space; (b) “fuzzy” set-theoretical models, describing the polysystem units of landscape-zonal organization by operations with the ecological niches as descriptive vectors. Predictions of ecosystem transformations include two stages of analysis: (1) evaluation of the probabilities of changes in the functional states of ecosystems and (2) calculations of the rates of ecosystem transformations. Quantitative predictive analysis is carried out by means of operations with the hydro-thermal niches of zonal-regional ecosystems. The ecological estimates of forthcoming global warming refer first of all to the functional but not structural-morphological prediction. The most probable directions and degree of conversion of the ecosystem are estimated by the maximum values of transformation. The algorithms of predictive calculations are described in detail for both stages of analysis. The results of the zonal-regional prognostic analysis are presented in both graphic-analytical models and small-scale maps.

Keywords: Landscape-zonal Systems; Contemporary Global Warming; Information and “Fuzzy” Set-Theoretical Models; Predictive Empirical-statistical Modeling and Mapping

ARTICLE INFO

Received: 24 April, 2023
Accepted: 20 June, 2023
Available online: 28 June, 2023

COPYRIGHT

Copyright © 2023 by author(s).
Natural Resources Conservation and Research is published by EnPress Publisher LLC. This work is licensed under the Creative Commons Attribution-NonCommercial 4.0 International License (CC BY-NC 4.0).
<https://creativecommons.org/licenses/by-nc/4.0/>

1. Introduction

Fundamental problems of ecology and geography include, as is known, the problem of global changes, which is the core of the “International Geosphere-Biosphere Program”^[1]. The Program is designed for a long-term outlook and envisages the development of scenarios for the nearest future of the biosphere in terms of physical models describing basic processes and events. One of the most dynamic natural processes on the planetary scale, which efficiently influenced biosphere evolution in the past and determine its condition in the future, are changes in the global climate caused by the changed chemical composition of the atmosphere, with the corresponding demonstration of the

greenhouse effect. The coming global climatic changes will be associated first of all with technogenic growth of the content of CO₂ and other greenhouse gases in the atmosphere, which may disturb the natural carbon cycle in the biosphere and lead to large-scale ecological consequences, including reorganization of the landscape-zonal structure of entire continents.

Global biosphere processes and phenomena are understood the most profoundly at the level of ecological regions. Global geosystem monitoring is most up-to-date and realizable on the scale of individual ecological regions as well^[2]. However, natural processes and events on the regional hierarchic level are characterized by the greatest diversity and high discreteness^[3], therefore, the regional response of global climatic changes inevitably takes the form of multiple reactions of vegetation, soils, and landscapes as a whole to background climatic signals. So far there is no distinct notion of this multiplicity because the measure of the sensitivity of soil-biotic components to climatic changes in different zonal-climatic and geomorphological conditions has not yet been estimated. The regional level of geo-ecological prognoses still has not been developed enough due to the insufficiency of factual material and methodical difficulties of the transfer of hydro-climatic prognosis from the global level to regional.

The regional response to global climate change involves the multivalued response of vegetation, soil, and the entire landscape to background climate signals. There is still no clear understanding of this ambiguity since the measure of the sensitivity of soil-biotic components to climate change in various zonal climate conditions has not been assessed. The currently known achievements in environmental forecasting are rather sketchy^[4-6].

One way to solve the problem of the poorly developed level of geo-ecological forecasts is to create a unified regional paleo-forecasting concept. Based on the example of the Volga River basin, short-term landscape-ecological scenarios were proposed for the biosphere, along with their paleogeographic counterparts, as a unified system of global changes in the natural environment. Special attention was paid to the mechanisms of shifts in the mosaic of

geo(eco)systems for given signals of perturbing impacts to the climate system anticipated in the foreseeable future (before the middle and end of the 22nd century) and their counterparts that could have occurred in the geological past, in the optima of the Mikulino (Eemean) interglacial (120–130 ka ago) and Holocene (5–7 ka ago). To record these mechanisms, regional analytical frameworks and cartographic (on a much larger scale than has been done before now) predictive models of landscape-ecological conditions have been developed, as well as models of two specified paleo-geographic sections in light of future and past changes in the global climate.

Ecological safety of large territorial subunits of the continental biosphere significantly depends on the state of the zonal-regional types of natural ecosystems, first of all, forest cover. Therefore, the problem of maintenance of forest ecosystems and reproduction of forest resources on the southern boundary of the temperate forest zone, where forest communities are present in the states close to critical, is among the fundamental ecological problems. That is why in this article we will pay attention to climate-genic changes in the forest cover of lowland and mountainous territories.

2. Peculiarities of geo-ecological prognoses

Problems of the predictive dynamics of forest ecosystems in a changing climate have been studied very little. The well-known imitational models of forest responses to climate impacts, which we considered in^[7], correspond to narrow specified limits of habitat conditions. Therefore, the results of such modeling are insufficient for forecasting the state of the entire forest community as a whole and do not encompass the spatial diversity of its successive shifts with the same background impact. The regional landscape-ecological forecast developed by the author constructs discrete empirical-statistical models of natural ecosystems^[8], which makes it possible to work with a relatively small number of the most informative features and obtain results less defined time-wise, but with a higher spatial resolution than with imitation modeling (see below).

The given article expands on the principles of regional landscape-ecological prognosis developed by the author, which is based on the methods of the theory of information, descriptive (“fuzzy”) sets, and Markovian chains^[7]. These methods are used for numerical paleo-reconstructions for the first time. The ways and efficiency of using these principles in the assessment of the past and future states of natural ecosystems are demonstrated as well.

Hydrothermal trends up to 2100–2200 are based on two global models of the general atmospheric circulation family AOGCMs (see below).

The simulation tool was the previously developed method of regional geo-ecological prediction^[7,9]. The mechanisms of evolutionary processes were revealed by the trajectories of functional-structural transformations of bio-geosystems and landscapes in light of the given hydrothermal trends for a particular period of climate prediction, with predetermined temperature and precipitation deviations from the base period (for approximately 100 years till 1985). The probabilistic character of the landscape-ecological prediction made it possible to reveal the local and regional diversity of responses of geo(ecosystems) to the same background climatic signal, their stability, as well as the trajectories of their mutual and extra zonal transitions, being a multivalued pattern of climate-genic mechanisms of evolutionary processes.

The known simulation models of forest responses to climatic impacts^[10–12] meet the narrow-preset framework of habitat conditions, therefore the results of such modeling are insufficient for prediction of the state of forest community as a whole and do not cover the spatial diversity of succession changes under the same background influence. The local and regional landscape-ecological prediction, which we have developed, is based on the construction of discrete empirical-statistical models of natural geo(ecosystems)^[7,8,13]. They are used to obtain probabilistic prognostic estimates of the behavior of regional landscapes and biogeocoenoses under various geomorphological, zonal-climatic, and edaphic conditions of specific ecoregions. These models describe the category of self-organizing systems, which can adequately describe stabilizing selection as a response of the biota to climatic perturbations

exceeding the adaptation threshold. In these models, the results of field observations are used as an empirical basis for modeling itself, rather than as reference data for testing results of calculations. This, first, minimizes the effect of the subjective factor in developing the model; second, provides a considerably higher spatial resolution than, e.g., simulation modeling; and, third, gives empirical grounds for wider geographic generalizations.

All predictive ecological models proceed somehow or other from the principle of actualism; however, they are unambiguously determined in some cases and probabilistic in other cases. The determined models do not take into account the diversity of states of subregional and local geo(ecosystems) under the same background climatic conditions, which is especially typical of mountain territories. Ecological-geographical prediction is always more reliable and practically significant if it is characterized by certain stochasticity, diversity, i.e., if it is probabilistic.

The strategy of the landscape-ecological prognosis was as follows: first to carry out an identification of picked out ecosystem objects (either zonal types and regional kinds of landscape or local nature complexes) to certain values of contemporary climatic conditions, and then to make an estimate of the most probable transformation of revealed ecological niches of given objects according to expected climatic changes for given prognostic date. Predictions of ecosystem transformations include two stages of analysis: (1) evaluation of the probabilities of changes in the functional states of ecosystems and (2) calculations of the rates of ecosystem transformations. Quantitative predictive analysis is carried out using the operations with hydro-thermal niches of regional or local ecosystems. The algorithms of predictive calculations are described in detail for both stages of analysis. In conclusion, the methods of calculation and construction of average weighted (by territory) matrixes and or-graphs of landscape-ecological transitions (for prognosis) and deviations (for paleo-reconstruction) have been considered.

The principle of the functional isomorphism of ecosystems proposed by us is used for the correction of the net of functional-structure transitions. The

models of functional isomorphism bring significant restrictions in the probability pattern of predicted trajectories of changes in geo(eco)systems, and this pattern becomes more ambiguous and ordered. The foci of transition networks are maximally isomorphic binary links—correlation pleiades of the highest level of similarity of bio productive niches; they form priority chains of soil-phytocoenological transformations.

The results of the regional prognostic analysis are presented in both graphic-analytical models and large-scale maps. The transition from the local to the regional level of prognostic modeling is carried out using inductive hierarchic extrapolation, a method that we developed based on the empirically established phenomenon of polyzonal nature of local ecosystems as a response to global climate changes^[14].

It has already been attempted to simultaneously apply the “micro-” and “macro-substrate” approaches to landscape analysis, which is a merely landscape-ecological problem. As is known, landscape ecology applies to the interrelationship between the “ecological processes” underlying landscape heterogeneity and the landscape “pattern” formed at much larger scales than these processes^[15].

The ecological-geographical forecasts can only be probabilistic^[16,17]. We proceed from the premise that “... the numerical predictions of prognostic models ... should be considered ... rather as information for thinking about the likely future trajectories of ecosystems ... taking into account the significant uncertainty of forecasts”^[18]. The predictive modeling undertaken by us is fundamentally probabilistic.

The general principle of the prognosis is expressed in the following: the value of the climatic-caused transformation of one ecosystem into another is the greater, the lesser is the degree of intersection of their climatic niches in the initial states, that is, the greater are the contemporary contrasts of their functional states, and the larger will be the range of the overlap of niches after the rapprochement of ecosystems by the given climatic factor.

This principle corresponds to one of the main provisions of the ecology of communities. Intense competition between populations leads to the

transformation of the community itself in the direction that corresponds to a new state of the environment, according to the Gauze law of competitive exclusion^[19], provided that immigrant populations dominate local populations in their competitiveness.

For example, the transformation of object A into object B should be the greater, the more distant are their positions in the multidimensional ecological space and the closer do they become after object A has shifted in the coordinates of this space (given that the climatic niche of object B is unchanged). In this case, object A is a reductant and object B is an absorber. In turn, object B is transformed into object C, with the natural boundaries shifting accordingly, etc. As a result, the general picture of ecosystem transformations in the region is drawn.

By the maximum values of transformation, the most probable directions and the conversion degree of the ecosystem are estimated. At the same time, an unambiguous character of transformation of regional ecosystems is proposed at a fixed value of geophysical trend, when the new state may have features of not one but several states existing at a given moment.

In essence, a landscape-ecological prognosis for the nearest several decades (to 100 years) is functional rather than structural. Characteristic (typical) times of metabolic parameters are much smaller than those of morphological parameters of ecosystems^[20]. Changes in the rates of organic matter reproduction and decomposition occur within a period ranging from a few months to three to five years^[7,21,22], which is commensurate to the time of general shift in the climatic system itself. Thus, functional relaxation as the primary response of ecosystems to an external factor is a priority object of landscape ecological prediction. The main prediction based on ecological estimation of the forthcoming global climate warming is expected to be functional rather than structural-morphological.

The supposed functional-structural shifts in geo(eco)systems that can be determined by climate changes (in this case, anthropogenic changes), with a period of fluctuations of 50 years and more, characterize not the future natural complexes per se but rather the landscape-ecological conditions and, accordingly, the limit of ecological equilibrium, which

real bio-geosystems will tend to in their variations. The time of reaching this equilibrium calculated in the number of steps $\tau(s)$ or in the number of years $\tau(y)$ relates only to the functional relaxation but not to the full period of structural transformation. The latter will be determined not only by the intensity of external effect but also by the characteristic times of different natural attributes, according to Armand and Targul'an^[23]. For forest landscape, as is known, the prediction step not exceeding the lifetime of one generation of forest stands makes it possible to determine potential forest growth conditions.

The prognostic landscape-ecological analysis has been performed using a series of empirical models: (a) informational, serving as a basis for the regional and local banks of ecological niches of geo(eco)systems that characterize their parametric space; (b) "fuzzy" set theory, describing the polysystem unit of nature-territorial organization by operations with the ecological niches as descriptive vectors. Complex interconnections were revealed and the territorial ecological space of regional and local ecosystems was described based on information-statistical and fuzzy set-theoretical models.

Analytical models of landscape-ecological transitions were created by the empirical-statistical method described in studies of Kolomyts^[7,24]. As is known^[25], modern global warming began in the middle/end of the 80s of the XX century. Years 2050, 2100, 2150, and 2200 are the main predictive dates, for which the most probable degrees of deviation from the baseline (for 1985) functional states were calculated for individual geo(eco)ecosystems (both regional and local). Analogous deviations were calculated for geological past epoch—the optima of the Mikulino (Eemian) interglacial period (near 125,000 years ago) and the Holocene optima (5–7,000 years ago), which were considered as any paleo-climatic analogs of predictive periods. In these models, the weighted average influence of changes in temperature and precipitation (for the warm and cold seasons separately) and July stored soil moisture as well on the behavior of ecosystems was taken into account. The multitude of landscape-ecological transitions revealed in this way added important details to the general picture of changes in the structure of natural zonality shown in the prognostic maps of the region.

The procedure of predictive calculations included three stages: (1) establishment of the climatic niches of objects (in this case, landscape groups) in the space of modern and predicted hydrothermal parameters; (2) ordination of zonal vegetation, landscape, or biogeocoenotic units along the gradients of baseline climatic parameters, and (3) execution of operations with the niches based on their inclusion relations as descriptive vectors using methods of the "fuzzy" set theory.

Methods about the theory of fuzzy sets were applied to operations with the climatic niches of objects in the space of baseline and predicted hydrothermal parameters, with these objects being regarded as descriptive vectors. The probabilities of stabilization (stability measures) of each object and its functional transitions to other objects following the given climatic trend were found. The probabilities of stabilization (stability measures) of each object and its functional transitions to other objects following the given climatic trend were found. Then the network of transitions was rarefied by the principle of functional isomorphism of ecosystems^[7,9]. The final results of the calculations were weight-average (by the territory) matrices and oriental graphs of functional transitions of the plant or landscape units under consideration.

It should be noted that in case paleo-geographical models and maps reflect the disposition of landscape-zonal systems occurring in the past (in this sense, such models are equilibrium), the prognostic mapping assesses only a few equifinal states, to which these systems will tend in the course of first functional (metabolic) and then structural transformations under the action of climatic signals. Prognostic models are non-equilibrium, and zonal areas presented on them, as well as probabilities of transitions, indicate the landscape-zonal conditions, in which these ecosystems will function in the nearest decades.

3. Humidity factor and its significance for geo-ecological prognosis

The study of the impact of global climate changes on the structure and functioning of zonal-regional ecosystems would be expediently realized by

the example of marked and large biogeographical and landscape borders—ecotones. Such a border on the territory of Eurasia is a broad boundary strip of forest belt—boreal ecotone. Such a border on the territory of Eurasia is a broad boundary frontier between the boreal (mainly taiga-forest) and sub-boreal (forest-steppe and steppe) belts of plant formations. The frontier stretches from the Baltic Sea to the East Sayan and Baikal Lake and then, after a break, to Inner Mongolia. This transcontinental boreal ecotone

is a vector (connection) geosystem of the highest, or belt, rank. The main watershed of the Volga River basin is included in the boreal ecotone of the Russian Plain. **Table 1** shows the zonal-regional phytocoenological structure of this territory. This large territory, due to its natural peculiarities, has been a traditional object for the study of zonal forms of organization of geographical environment and become a basis for fundamentals of the theory of worldwide land zonality^[26–30].

Table 1. The classification scheme of primary plant formations of the natural zones of the East-European (Russian) plain, by Gribova *et al.*^[31]

Phytocoenological units			Groups of plant associations	
Zonal types and classes	Regional versions	Sub-zonal sub-types	Brief characteristics	Number and symbol
A. Dark conifer and broad-leaf—dark conifer forests (secondary aspen-birch)	East European (Upper Volga region)	Middle taiga	Spruce green mosses with small-shrubs	1 
		South taiga	Spruce small-shrub/grass	2 
		Sub-taiga	Broadleaf-spruce complex nemorose-herbal	3 
	Kama—Pechora—West Ural region	Middle and south taiga	Fir-spruce and spruce-fir grass-small-shrub, with green mosses, and grass	4 
		Sub-taiga	Fir-spruce complex nemorose-herbal	5 
			Broadleaf-fir-spruce nemorose-herbal	6 
B–C. Pine and broadleaf—pine forests (secondary aspen-birch)	East European (Upper Volga region)	Middle and south taiga	Pine, with spruce, green mosses with small-shrubs	7 
		Sub-taiga	Pine (with oak in undergrowth) small-shrub/grass	8 
			Broadleaf-pine and pine complex, with spruce	9 
		Forest-steppe and steppe	Pine and broadleaf-pine, with steppe undergrowth, and herbs-cereals	10 
D1. Broadleaf forest	East European	Northern forest-steppe	Lime-oak and oak	11a 
			Lime with admixture of other broadleaf kinds	11b 
D2. Typical and southern forest-steppe	Of the Pontic type	Typical forest-steppe	Meadow steppes with combination of oak forests	12 
		Southern forest-steppe	Rich herb-sheep's fescue-feather grass steppes, with oak Copses	13 
Northern steppe	Of the Trans-Volga type	Northern steppe	Rich herb-sheep's fescue-feather grass steppes	14 
Southern steppe	Of the Trans-Volga type	Southern steppe	Sheep's fescue-feather grass steppes	15 
Semi-desert	Of the Trans-Volga type	Semi-desert	Fescue-feather grass steppes in a complex with wormwood on salt licks	16 
Desert		Northern desert	Wormwood groups	17 

The ratio between radiation heat and atmospheric humidity, as is known^[28,32–34], is the most important landscape-forming factor responsible for the physiognomic traits of natural-territorial habitats (geo(eco)systems) of almost all structural levels of the biosphere—from global to local (topological). Along with that, this factor is the main link between these complexes and the biological cycle, which characterizes the functional aspect of landscape organization. The most comprehensive view of the hydrothermal regime of natural complexes is given by the atmospheric humidity factor as a landscape-geophysical parameter that reflects primarily the background climatic conditions of the territory. Quite some such factors are known: the annual and seasonal coefficients of the heat-to-humidity ratio proposed by Köppen, Vysotsky and Ivanov, Budyko, Bazylevych, Thornthwaite, Marthonn, Ryabchikov and Mirkin, Selyaninov, and Richter. In the present work, we have used Vysotsky-Ivanov’s annual atmospheric humidity factor F_{hum} . Recall that this coefficient is a ratio of annual precipitation r_{ann} to evaporativity E_0 (potential evapo-transpiration):

$$F_{\text{hum}}(1) = r_{\text{ann}}/E_0 \quad (1)$$

The values of E_0 parameter are calculated for each month:

$$E_0(\text{month}) = 0.0018 \cdot (25 + t)^2 \cdot (100 - w) \quad (2)$$

where $E_0(\text{month})$, t , and w are the month values of evaporativity, temperature, and relative air humidity, respectively. The Vysotsky-Ivanov’s annual atmospheric humidity factor is widely used in Russian hydrometeorology and physical geography. Firstly, this parameter allows the landscape-ecological analysis of territory based on the known information about the connections of global and regional geo(eco)systems and their components with the heat and humidity ratio. Secondly, it is the most suitable for calculations, because it is based directly on the data of long-term observations at meteorological stations.

According to our estimations for the territory of the Russian (East European) Plain, parameters E_0 and $F_{\text{hum}}(1)$ are formed mainly by the mean July temperature (t_{July}) with high correlation (R) and determination (R^2) factors:

$$E_0 = 1384 - 161.6 \cdot t_{\text{July}} + 6.245 \cdot t_{\text{July}}^2; R = 0.93; R^2 = 0.87 \quad (3)$$

$$F_{\text{hum}}(1) = 12.09 - 0.9095 \cdot t_{\text{Jul}} + 0.01744 \cdot t_{\text{July}}^2; R = 0.94; R^2 = 0.88 \quad (4)$$

The global climate prediction models are widely used for both planetary- and regional-level ecological forecasts, as they generally describe the hydrothermal trends by two initial parameters: temperatures and precipitation, which are predictors for the calculation of $F_{\text{hum}}(1)$. In these forecasts, the annual atmospheric humidity factor is usually compared with the zonal types/sub-types of plant formations and their longitudinal-sectoral variants^[3,28,35]. The tightness of these connections is rather high. For instance, for the zonal spectrum of the central part of the Russian Plain (from middle taiga to southern steppe), we have obtained an explicit deterministic series of distribution of the groups of primary plant formations by the gradient of the annual atmospheric humidity factor (**Table 2**).

Statistical analysis revealed highly significant correlations between positions of zonal (sub-zonal) boundaries and the F_{hum} parameter^[7]. For the western and eastern sectors of the Russian Plain, the boundary values of the annual atmospheric humidity factor are equal:

	West	East
Middle taiga	>1.88	>1.62
Southern taiga	1.88–1.63	1.62–1.35
Mixed forests	1.63–1.22	1.35–1.00
Broadleaf forests	1.22–1.09	1.00–0.97
Typical forest-steppe	1.09–0.90	0.97–0.75
Northern steppe	<0.90	<0.75

Covariance is $\leq 4\%$ – 6% , and only for the boundaries of the forest-steppe zone, it is up to 10% – 11% . These correlations were used for making a prognostic map of natural zones (subzones) in the region on the basis of the respective prognostic $F_{\text{hum}}(1)$ maps (see below).

The annual atmospheric humidity factor corresponds to the hydrothermal conditions of flat-interfluvial low-dimensional natural complexes—landscape facies, or biogeocoenoses^[21], as local represen-

Table 2. Ecological optimums (X) and periphery parts of climatic niches (●) for groups of plant formations on the headwater of the Volga River basin at the space of the values of annual atmospheric humidify factor (F_{hum})

Graduations of F_{hum}	Groups of plant formations (see in the Table 1)															
	1	4	7	2	3	5	8	9	6	10	11	13	12	14	15	16
0.50–0.61														●	X	X
0.61–0.73													●	X	X	●
0.73–0.82											●	●	X	X	●	
0.82–0.96										●	X	X	●	●		
0.96–1.04								●	X	●	X	●	●			
1.04–1.12						●	●	X	X	●	●					
1.12–1.23						X	X	●	●	●						
1.23–1.33			●	●	●	●	X			●						
1.33–1.45			X	X	X	●	●									
1.45–1.55		●	●	X	●	●	●									
1.55–1.65	●	●	X	●	●											
1.65–1.75	●	X	●	●												
1.75–1.85	●	X			X											
1.85–2.00	X	●			●											
Standard of F_{hum}	1.80	1.73	1.47	1.42	1.54	1.23	1.21	1.12	1.07	1.07	0.94	0.90	0.80	0.72	0.62	0.57

Foot-note: Matrix was made up by the results of informational-statistical analysis of the interrelations^[7,9].

tatives of the zonal-regional bioclimatic background of the given territory^[3,33]. This elementary unit of geographical ecology accepted in Russia corresponds to categories “Site”, “Eco element”, and “Land type phase” by classifications of Australia-Britain, Canada, and the USA.

On this level, however, there is also a broad range of extra zonal topo-ecosystems, which can simulate other zonal types of geographic environment, not only neighboring but also rather distant. Such ecological deviations from flat-interfluve natural complexes are formed under the influence of local geomorphological and edaphic factors refracting the given climatic background. Primarily, there are localized changes in “expense items” of the water balance: total evaporation and runoff, which creates the local structural and functional diversity of topo-ecosystems. That is why the connections between local geo(eco)systems and the t_{July} , r_{ann} and $F_{hum}(1)$ parameters are very weak and often statistically unreliable.

Thereby, it is necessary to find a factor of heat and humidity ratio that would adequately show the topological differentiation of the natural environment and could be used as the initial hydrothermal predictor for local landscape ecological forecasts. Such forecasts are especially relevant in light of the

modern and upcoming global climate changes. As is known^[36], the origins of global environmental changes lie on the level of elementary structural units of the biosphere. In the present work, we have presented some results of the scientific search in this particular field.

4. Numerical methods of regional geo-ecological prognoses and paleo-reconstructions

4.1 General calculation scheme

The regional and topological forecast analyses of climate-induced transformations of natural complexes described below are based on the numerical landscape-ecological forecasting method-logy developed by the author. The technique has been brought to the prescribed level and can be included in the scientific and methodological arsenal of geographical ecology. It organically combines a fairly rigorous formalized approach to solving forecasting problems and procedures for collecting, processing, and analyzing empirical material accessible to a wide range of researchers. In contrast to the well-known domestic and foreign approaches, this method provides for the multiple nature of the transformation of

natural complexes for a fixed climate trend. Two types of predictive models have been developed: choro metric and chronometric, which represent regional and local scenarios of climate-induced changes in the natural complexes of the Russian Plain and Greater Caucasus, including its highlands.

A significant feature in the methodology of ecological and geographical forecasting is its experimental character. Computational models reproduce the variation in predicted processes by empirically imitating the spatially distributed parameters of the basic ecological niches of the studied objects. The researcher sets the input variables and at the output obtains the pattern of predicted structural and functional states of the studied objects in this statistical sample, with the identification of new objects outside the sampling. In particular, the following were used:

- local empirical imitation of a regional bioclimatic trend using models of binary hydro- and thermo-edaphic ordination of forest topoecosystems;
- empirical imitation of climate-induced changes in the biological cycle based on hydrothermal ordination analysis of its parameters;
- empirical imitation of changes in productivity and the carbon sink in forest ecosystems during climate fluctuations.

Estimation of the ecosystem states and their most probable dynamic trends in terms of competitive relationships of their ecological niches are crucial for ecological prediction. This approach is based on the well-known presentation of the ecological niche of an object as a region of the distribution of its states in the given ecological space^[20]. Probabilistic landscape-ecological prediction involves operations with the current and expected hydrothermal niches of ecosystems^[7]. For this purpose, each of these niches was represented in the form a row (descriptive) vector—a “fuzzy” set of the states of phenomenon A caused by the given factor B . The row vector consists of standardized partial association coefficients:

$$C(a_i/b_j) = \frac{p(a_i/b_j)}{p(a_i)} \quad (5)$$

It is agreed that the association between a_i and b_j is significant at $C(a_i/b_j) > 1$. The higher is the probability, the greater is the coefficient; therefore, the components of row vector $C(a_i/b_j)$ are considered as “weighting” coefficients. Normalized partial coupling coefficients $C(a_i/b_j)$ regarded as weight coefficients were the components of the vector. Each of these coefficients is the equivalent of the probability (occurrence) of a specific object at a given gradation of the geophysical parameter. This probability is the higher, the higher the partial coefficient of the relationship.

The forecast strategy initially identifies phyto-coenotic, soil, or landscape units for certain values of the basic climate conditions and then quantitatively assesses the most probable transformations of these objects following anticipated climate change for a specified period. Since the probabilistic ecological forecast is conducted by operations with modern and assumed hydrothermal niches of geo(eco)systems, each such niche is represented as a fuzzy (descriptive) set of system states^[37] in the form of a row (or column) vector. The vector components are the normalized partial coupling coefficients $C(a_i/b_j)$.

The procedure of analytical prognosis involved (1) ordination of zonal vegetation units along the gradients of baseline climatic parameters and (2) quantitative assessment of the most probable transformations of these units under the effect of climatic changes expected within the period of interest. By transition, we mean a change of the functional and, then, structural state of an object such that the object assumes (at a certain probability) characteristics of other prototype objects, because, as its ecological (in the given case, hydro-edaphic) niche changes, it increasingly overlaps the niches of these objects.

According to the proposed principle of landscape-ecological forecasting, the climatically determined functional transformation of one geo(eco)system into another is the more significant, the smaller the degree to which their climate niches intersect in the initial state. The transformation of, say, object A into object B should be greater, the further these objects are separated from each other in the multidimensional ecological space and the closer they will be resulting from the shift of object A over the

coordinates of this space. Here, object A is a decomposer, and object B is an absorbing agent. In turn, object B transforms into object C with a corresponding shift of natural boundaries, etc. As a result, the general pattern of geo(eco)systemic transformations in the region emerges.

The ecological niches of a particular subdivision (state) of a phenomenon in the set of states of a given factor were determined with binary ordination of the phenomenon. To this end, in all states a_i of phenomenon A with their prior $p(a_i)$ and conditional $p(a_i/b_j)$ probabilities, the partial coupling coefficients $C(a_i/b_j)$ were calculated (see Equation (5)).

The matrix of these coefficients describes the system of climate niches of phytocoenoses, soils, or landscapes in the space of changes in a given hydrothermal parameter. Then, the positions of each vector of ecological niches of the phenomenon were normalized to obtain specific frequencies $C(a_i/b_j)$ ($\sum C(a_i/b_j) = 1$). Gradations of the factor with maximum values $C(a_i/b_j)$ form a certain optimal region of the phenomenon, it's ecological dominant, while the remaining gradations belong to the "fuzzy" part of the niche.

The mechanism of estimation of the probability of ecosystem transitions (both for forecasts and paleo-reconstructions) is illustrated by Venn's diagram (Figure 1). Here, A_0 and A_1 are respectively an initial (contemporary) and final (future) values of the row vector of the ecological niche of object A (either landscape group or facie group) \bar{a} which must be absorbed by another object B if its niches intersect each other in the final state more than in the initial state. The landscape-ecological transition proceeds in direction $A \rightarrow B$ and the absorption proceed in the opposite direction $B \rightarrow A$. The shaded area $a + b + c$ on the diagrams reflects the total value of transformation of object A which can be expressed in terms of the following measure of inclusion, by Andreev^[37]:

$$a + \epsilon = A_0 \cap A_1; \epsilon = A_0 \cap B_0; \epsilon + c = A_1 \cap B_0. \quad (6)$$

where, " \cap " is the sign of intersection (logical product) of two sets. The elements of the intersection "zone" belong to two sets simultaneously.

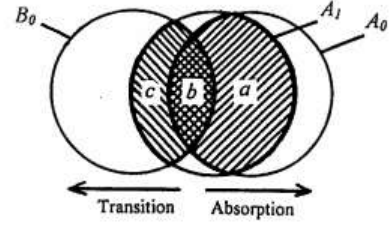


Figure 1. Venn's diagram, illustrating the mechanism of probability estimation of landscape-ecological transitions (explanation in the text).

It is supposed that any object A must be absorbed by another object B if its niches intersect each other in the final state more than in the initial state. Initial (contemporary) A_0 and final (future) value A_1 of the row vector of the climatic niche of object A are considered. For each pair of objects A and B , two predictive characteristics were calculated: $P_{ii} \equiv K(A_0 \rightarrow A_1)$ is the transition of object A into itself (the probability of its stability), and $P_{ij} \equiv K(A_0 \rightarrow B_0)$ is the probability of its absorption by another object B (" \equiv " is the identity sign). These characteristics were expressed as the following measures of inclusion (" \cap "):

$$K(A_0 \rightarrow A_1) = \frac{A_0 \cap A_1}{A_0} \quad (7)$$

$$K(A_0 \rightarrow B_0) = \frac{A_1 \cap B_0 - A_0 \cap B_0}{A_0} \quad (8)$$

Transitions characterize the degree of the most probable deviation of the functional state of a given ecosystem from its current state for a given forecasted or paleogeographic period. Since operations are carried out with descriptive sets, the calculation formulas, according to Syomkin^[38], take the form:

$$K(A_0 \rightarrow A_1) = \frac{\sum_1^{NP} \min[L_i(A_0), L_j(A_1)]}{\sum_1^N L_i(A_0)} \quad (9)$$

$$K(A_0 \rightarrow B_0) = \frac{\sum_1^{PQ} \min[L_j(A_1), L_k(B_0)] - \sum_1^{NQ} \min[L_j(A_0), L_k(B_0)]}{\sum_1^N L_i(A_0)} \quad (10)$$

Here i , j , and k are the ordinal numbers of the partial coupling coefficients in the vectors describing the ecological niches A_0 , A_1 , and B_0 , respectively, and N , P , and Q are the total volumes of the corresponding vectors.

To distinguish the interpretation of the results of

predictive and paleogeographic calculations, let us agree to call the first landscape-ecological transitions, and the second, deviations of the past states of geo (eco-)systems from their current state.

Thus, a specific quadratic matrix of probabilities of stabilization of each object (diagonal elements of the matrix, P_{ii}) and its transitions into other objects (P_{ij}) is obtained for each prediction period. Here, the zero and negative values of probabilities are possible. The former indicates the absence of transitions and the latter show intensification of the contrast between the functional states of objects (at $A_1 \cap B_0 < A_0 \cap B_0$). Further operations are executed with the transition probability matrices. All negative transitions are provisionally replaced by zeros.

If objects A and B are first-order neighbors, then the value of displacement of the boundary between them in the $A \rightarrow B$ direction is taken as proportional to the calculated measure of transformation of object A . In its turn, object B can be transformed into the following objects (D , C , etc.). The evolution of ecosystems is usually multivariate; hence, all possible transitions have to be considered for each of them with revealing the maximum measures of transformation, which will indicate the most probable directions of transformation of landscaped or phytocoenological structures as a whole. For first-order landscape neighborhoods, this process will be rather distinct if $P_{cn}(B) > P_{cn}(A)$, i.e., given that absorbing object B has a higher power of climatic niche P_{cn} compared to absorbed object A .

Graphical-analytical models (see below **Figures 2** and **3**) show the probabilities of landscape-ecological transitions for the prognoses and the probabilities of deviations for the paleo-reconstructions.

The developed technique made it possible for the first time to calculate not only the probabilities but also the rates of functional transformations of biogeocoenoses, landscapes, and plant formations, yielding predictive estimates with a set lead time. This is the second stage of forecasting and paleogeographic calculations. Using the methods of the theory of finite Markov chains, the potential rates of transformations of climatic niches of geosystems were determined, which made it possible to arrive at predictive estimates with a given lead time. For the

simulation, discrete first-order Markovian chains with a short “memory” of one prediction step, during which the process is considered stationary, are used.

It was possible to calculate the overall probability P_i of transformations of the absorbing-agent object, the total M_i and partial m_{ij} rates of its transitions to all j th absorbing-agent objects, and the time $T(P_{ii})$ of the total transformation of the decomposer, expressed as the number of steps (d) or as years. According to the model of W. Krumbein, the calculated formulas of these characteristics have the form^[39]:

$$P_i = (1 - P_{ii}); M_i = (1 - P_{ij})/d; m_{ij} = P_{ij}/P_i; T(P_{ii}) = 1/M_i \quad (11)$$

Here, d is the number of steps. The rates h_{ij} (and consequently times) of transitions are defined by way of a non-complicated algebraic transformation of the initial normalized matrix of transition probabilities where both the relative transition probabilities (P_{ij}) and the a priori probabilities (P_i).

By multiplying of value $t(P_i)$ into the time equivalent of the first step (70 years in our case), we obtain the expected absorption time (in years) which makes conceptually the final time of full transformation of the given landscape climatic niche. Next it is essential to calculate h_{ij} , which is an absolute partial rate of transition of i -landscape niche to j -niche (as a conditional probability). This rate is equal:

$$h_{ij} = m_{ij} \cdot M_i \quad (12)$$

Values h_{ij} are calculated on all lines of matrix P_{ij} (except its diagonal elements). The relation h_{ij}/M_i , shows us that part of the total one-step reduction of the niche property of i -landscape kind (for example, area or the part of any other attribute of transformation) accounts for the transgression of j -kind niche. It is thereafter an easy matter to calculate what part of properties of the given landscape kind will be absorbed by other kinds at time intervals (steps), those are either 25, 40, or 70 years.

On matrices of parameter h_{ij} , the prognosis landscape-ecological maps were compiled. They show areas of future equilibrium states of vegetational cover which correspond to equifinal stages of the exo-dynamic phytocoenosis successions. However, the terms of the onset of these states remain

unknown, and its definition is an independent geobotanic problem. The prognosis maps present two dynamic characteristics simultaneously: 1) prevailing tendency of transitions of the niche of the given group of plant formation from “its” natural zone

(subzone) into the formation niche of other zones; 2) common degree (or rate) of interzonal transformation of the climatic niche of the given phytocoenological group.

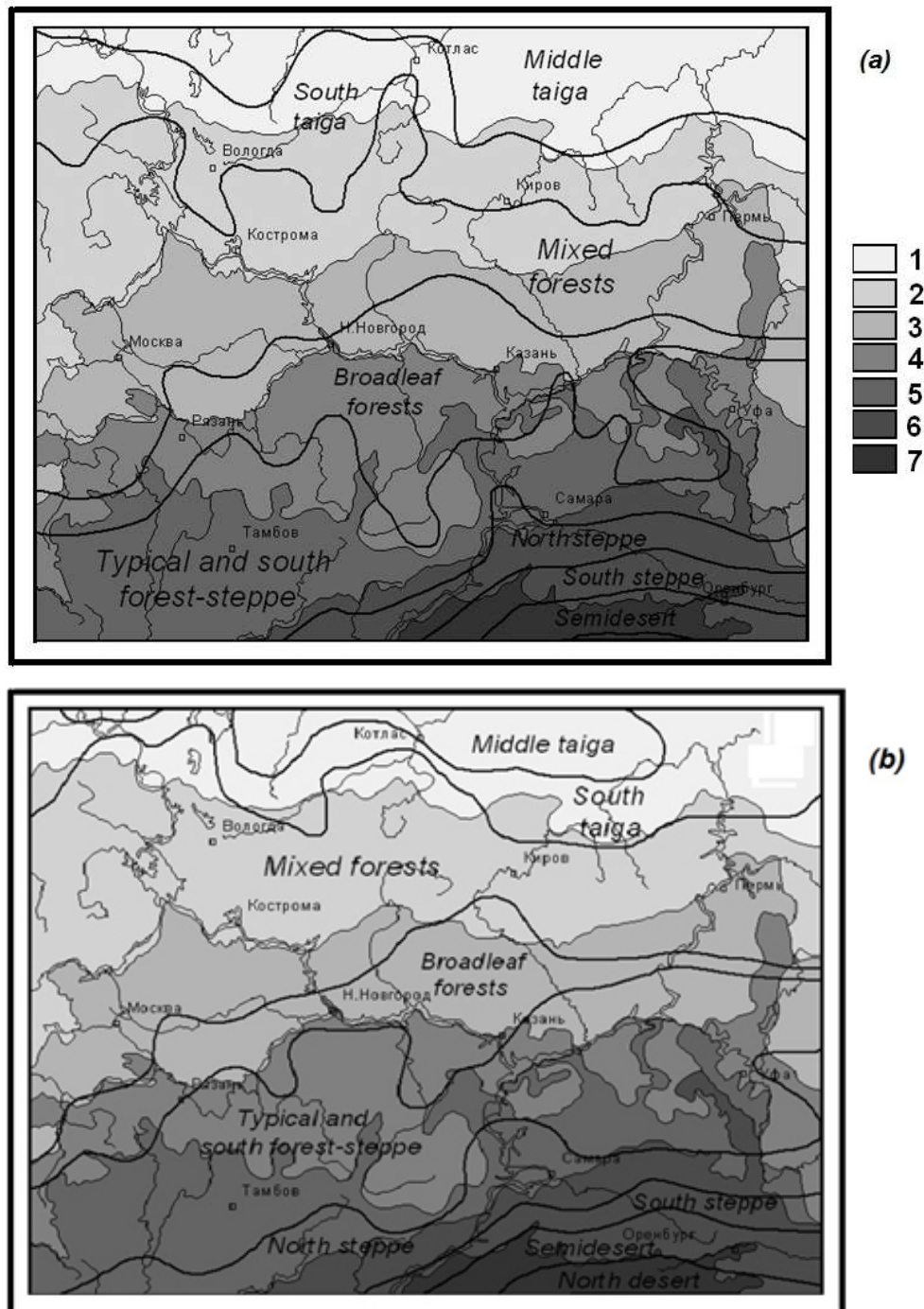


Figure 2. Prognosis of changes in the landscape-zonal structure of the Volga River basin and its surrounding for the periods to years 2050 (a) and 2100 (b), according to GISS model. The shaded areas indicate the areas of modern natural zones and sub-zones: 1 and 2—middle and southern taiga; 3—mixed forest (sub-taiga); 4—broadleaf forests; 5—typical and southern forest-steppe; 6—northern steppe; 7—southern (dry) steppe.

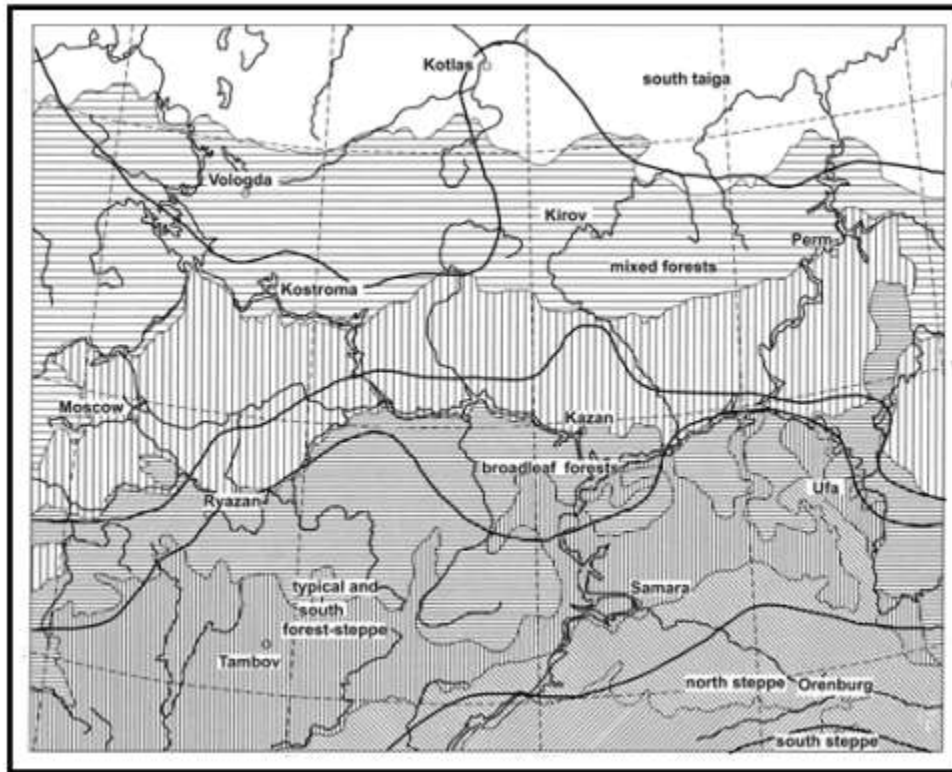


Figure 3. Zonal landscape-ecological conditions of the Volga River basin and its encirclement for the paleo-reconstruction for Mikulino (Eemian) interglacial optimum. Conventions meaning of modern natural zones and sub-zones are as in **Figure 2**.

Both mentioned above characteristics are well represented in the legend to the prognosis maps of landscape-ecological conditions.

Climate forecasting scenarios up to 2150–2200 served as regional hydrothermal signals based on global models of the AOGCMs family: the extreme HadCM3, version A2^[40,41], and the more moderate E GISS^[42,43], with earlier version GISS-1998. By our order in 1993, Menzhulin and Savvateev^[44] developed a regional version of the global GISS model (for the territory of the Russian Plain), with a spatial resolution of 1° latitude and longitude. This made it possible to carry out calculations and predictive computer mapping of the entire complex of hydroclimatic conditions of the Volga River basin and its surroundings on a scale of 1:3,500,000.

The second E GISS model quite realistically displays the past centennial climate dynamics for the European continent. It simulated quite well the observed changes in the global climate for the period 1880–2003, and especially over the last 3–4 decades. It quite realistically reflects the centennial climatic dynamics within the European continent. The model describes an increase in global temperature by 2.7–

2.90 with a doubling of CO₂ concentration in the atmosphere, which corresponds to the empirical range of climate sensitivity established from paleogeographic data^[43].

According to the HadCM3 model, we divided the entire forecast period into five stages (steps): 1985–2025–2050–2075–2100–2150. For the GISS-1993 and E GISS models, four stages are distinguished: 1985–2050–2100–2150. The basic period is considered to be the period of instrumental meteorological observations in 1881–1985, from the end of which the modern global anthropogenic warming began^[10].

4.2 Algorithm of analytical calculations

The procedure of the first stage of own prognosis analysis for regional landscape structure consisted of the following operations^[7,24,45].

(1) Using the information analysis of connections on each object (landscape group) with that or another climatic characteristic two matrices of partial association coefficients ($C(x_i/y_j)$) were obtained: matrix T_0 for the base period and matrix T_1 for the given prognostic dates. The graduations of the given factor are presented on the columns of each matrix and the

gradations of the given object are presented on the lines. Since the regional climate prediction is differentiated concerning temperature and precipitation, we have formed 4 pairs of matrixes: on the mean January and July temperatures ($T_0(1)$ and $T_1(1)$; $T_0(2)$ and $T_1(2)$); and on the atmospheric precipitation of cold and warm periods ($T_0(3)$ and $T_1(3)$; $T_0(4)$ and $T_1(4)$).

(2) The above formulas were used to calculate four square matrixes $T(1)$, $T(2)$, $T(3)$, and $T(4)$ of the measures of stabilization (resistant stability) P_{ii} of each i -th object (diagonal matrix elements) and measures of its transformation P_{ij} into other j -th objects. Zero values of matrix elements show the absence of a transition in the given pair of objects, and negative values point to the intensification of contrast between them ($A_1 \cap B_0 < A_0 \cap B_0$).

The P_{ii} and P_{ij} parameters represent the two alternative categories of *geo(eco)system stability*: *areal* (geotopic) and *migration* (transgressive), which characterize the state of stable equilibrium of the system and its forced behavior as a response to external effects, respectively.

For simplification of predictive calculations, the above condition $P_{cn}(B) > P_{cn}(A)$ is not taken into consideration at the given stage of described algorithm development, which certainly reduces the reliability of results.

(3) Account was to be taken of simultaneous changes of all four (or three) cited climatic factors, then, based on matrixes $T(1)$, $T(2)$, $T(3)$, and $T(4)$, the first factor-weighted average matrix T_{wa} of object transformation was calculated. The “weighting” coefficients for its calculation were values of parameter $C(X;Y)$, which were normalized once again to obtain a linear polynomial of dependencies between the distributions of objects and the geophysical factors under consideration. For example, the revealed values of the normalized coefficients of the couplings of the groups of plant formations of the Volga River basin with the basic climatic conditions made it possible to obtain for calculating the matrix $T_{wa}(1)$ a linear polynomial with the following “weight” coefficients:

$$T_{wa}(1) = 0.131 \cdot T(1) + 0.388 \cdot T(2) + 0.147 \cdot T(3) + 0.334 \cdot T(4) \quad (13)$$

For the groups of regional landscapes of the given region of Greater Caucasus prognostic calculations matrix $T_{wa}(1)$ were counted on the linear polynomial with the following coefficients:

$$T_{wa}(1) = 0.241 \cdot T(1) + 0.315 \cdot T(2) + 0.126 \cdot T(3) + 0.318 \cdot T(4) \quad (14)$$

(4) At this stage of operations with the matrixes, it is necessary to take into account the probable presence of “residual” transitions of some or other objects into other prototype objects absent in our operational system (sampling), i.e., to extra-sampling objects. For some facial groups, these transitions seem to be dominant and even unique. Such transitional “residue” $P_{ij}(x)$ for each object (i.e., for each line of the weight-average transition matrix) can be easily found from the ratio:

$$P_{ij}(x) = 1 - P_{ii} - \sum P_{ij} \quad (15)$$

The $P_{ij}(x)$ values are entered as an additional column into matrix T_{wa} . If the “residue” is negative, it means that all predicted transitions of the given object are in the limits of the considered set of prototype objects and there are no other transitions. Negative “residues” of transitions are changed for zeros.

(5) Comparable values of the probabilities of transition of some or other objects into different prototype objects can be obtained if the sum of these probabilities in each line of the matrix is equal to 1. After normalizing each of the five T_{wa} matrixes (with “residual” columns) by lines, we will obtain the second weight-average matrixes $T_{wa}(2)$. The lines of the matrix with positive transition “residues” prove to be normalized already at the preceding (4th) stage of calculations.

(6) In conclusion, the correcting procedure is performed. Matrix $T_{wa}(2)$ contains quite a lot of elements with very low (below 1%–2%) probabilities going beyond the limits of measurement and calculation accuracy. It is necessary to calculate the guaranteed minimum of probabilities of landscape-ecological transitions: M_{min} . The simplest method of finding the guaranteed minimum of elements is based on the application of the one-sided criterion of their significance, $t = s$, which provides the 5% level of significance. All values of M transitions or

deviations (P_{ii} or P_{ij}) below the difference of M —s must be eliminated. With this purpose, we calculate $M_{\min} = M - \sigma$ and drop all vector elements below this difference.

Thus, each object acquires a much shorter transition vector. Residual vector elements are normalized again and, thus, we obtain the third matrix of transition probabilities average weighted by the given geophysical factor: the $T_{wa}(3)$ matrix. It gives a rather clear notion of the potentials of transformation of some or other objects or, on the contrary,

their ability to resist external influence (**Table 3**). The orientate graphs of probabilities of functional transitions between the objects are plotted on the basis of $T_{wa}(3)$ matrices (**Figure 4**). These graph-analytical models are the main tool for landscape-ecological prediction. They give the most general notion of the exogenous succession dynamics of ecosystems as whole natural-territorial complexes.

An example of the results of the first and second stages of predictive calculations is presented in **Tables 4 and 5**.

Table 3. Volga River basin. Probabilities of stabilization of plant formation groups (P_{ir} —diagonal matrix elements, in bold) and their mutual transitions

(P_{ij}) for the forecast period of 2050, according to the forecast-climate model GISS-1993

															
	0.059	—	—	—	—	0.112	0.153	0.093	0.072	0.013	—	—	—	—	—
	0.049	—	—	—	—	—	—	0.047	0.082	0.099	0.104	0.071	0.049	—	—
	—	—	—	—	—	0.066	—	0.067	0.101	0.126	0.087	0.019	0.034	—	—
	—	—	—	0.161	—	—	—	—	0.032	0.096	0.094	0.094	0.104	—	—
	—	—	—	—	0.042	—	—	—	0.036	0.113	0.118	0.104	0.108	—	—
	—	0.042	—	0.058	0.066	0.067	0.039	—	—	—	—	0.051	0.107	0.103	—
	0.101	—	0.088	0.032	—	—	—	—	—	—	0.063	0.069	0.079	0.067	—
	0.041	0.032	0.084	0.037	0.026	—	—	—	—	—	—	—	0.085	0.098	0.098
	—	0.067	0.041	0.062	0.062	—	—	—	0.111	—	—	—	0.053	0.088	0.071
	—	0.083	0.056	0.076	0.086	—	0.046	—	—	0.249	—	—	—	—	—
	—	0.106	—	0.040	0.062	—	0.068	—	—	—	0.283	—	—	—	—
	—	0.015	—	—	0.049	0.056	0.017	0.083	0.038	—	—	0.1-4	0.018	—	0.118
	—	—	0.008	0.021	0.055	—	0.054	0.074	0.045	—	—	—	0.486	—	—

Direction of the transitions \longrightarrow

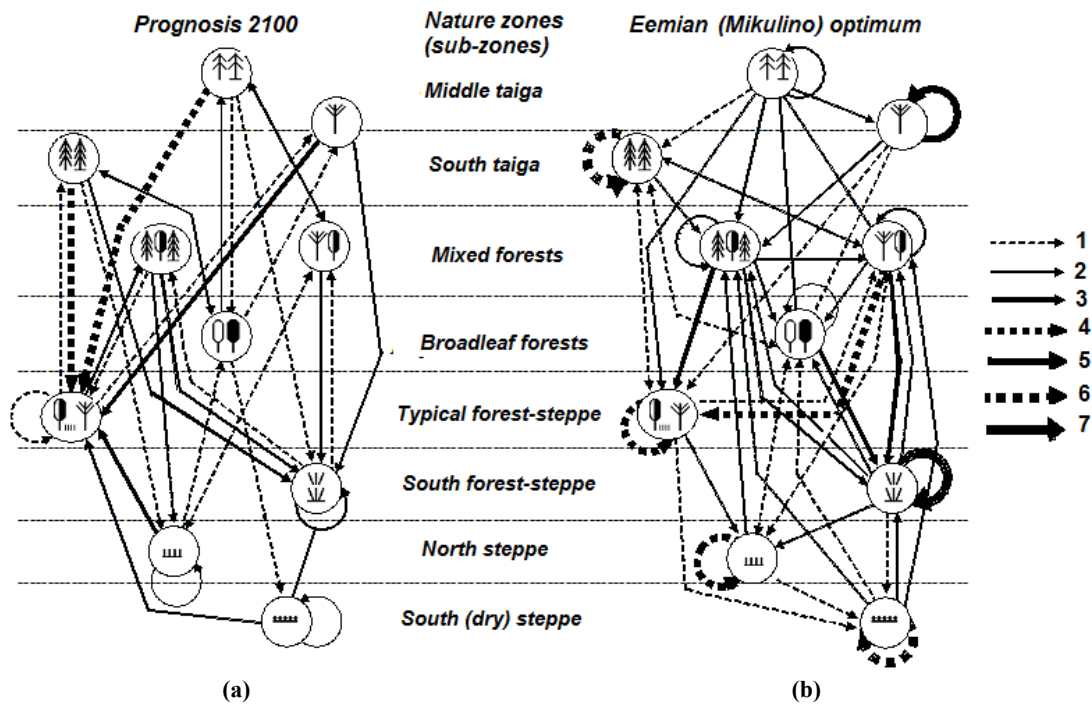


Figure 4. Vector graphs of the probabilities of functional transitions and deviations between the plant formation groups of the head-water of Volga River basin and its surrounding on the prognostic periods up to year 2100, according GISS model, and on the paleo-reconstruction for Mikulino (Eemian) optimum. Probabilities of inter-formation transitions and deviations: 1—0.20 and less; 2—0.21–0.30; 3—0.31–0.40; 4—0.41–0.50; 5—0.51–0.60; 6—0.61–0.70; 7—0.71–0.80.

Table 4. Volga River basin. Groups of plant formations. Characteristics of Markov's process (see in the text) for the prognosis date of year 2100

	P_{ii}	P_i	P_{ij} (mean)	M_i	τ (steps)	τ (years)	Sigma
	0.059	1.000	0.143	0.333	3.00	180.00	0.085
	—	1.000	0.200	0.333	3.00	180.00	0.075
	—	1.000	0.143	0.333	3.00	180.00	0.104
	0.161	0.966	0.143	0.322	3.10	186.27	0.071
	0.042	1.000	0.167	0.333	3.00	180.00	0.107
	0.067	1.000	0.143	0.333	3.00	180.00	0.047
	—	1.000	0.250	0.333	3.00	180.00	0.036
	—	1.000	0.200	0.333	3.00	180.00	0.106
	0.111	0.859	0.143	0.286	3.49	209.55	0.070
	0.249	0.952	0.143	0.317	3.15	189.10	0.051
	0.283	0.929	0.143	0.310	3.23	193.85	0.051
	0.134	1.000	0.167	0.333	3.00	180.00	0.038
	0.486	0.608	0.200	0.203	4.94	296.25	0.117
	0.415	0.727	0.143	0.242	4.13	247.54	0.145
	0.269	0.770	0.125	0.257	3.90	233.70	0.120

Foot-note: P_{ii} , the probability of stabilization of object i ; P_{ij} , the probability of its transitions into another object j ; P_i , the total probability of transitions of object i into all other objects; M_i —the total rates of transition from the given state in one step; τ (steps) and τ (years), the total time of object staying in condition P_{ii} expressed in the number of steps and in years; sigma (σ)—standard deviation.

Table 5. The generalized characteristics of probabilities and rates of functional and structural transitions for landscape groups of the northern macro-slope of Great Caucasus for the prognostic period of 2100, according to the thermo-arid climatic trend by E GISS

Altitudinal belt	Statistical parameters				
	P_{ii}	P_i	P_{ij} (mean)	τ (steps)	τ (years)
Piedmont	0.33–0.92	0.08–0.45	0.13–0.33	3.0–25.3	327–2830
Lower- and middle-mountain	0.39–0.75	0.25–0.61	0.11–0.14	3.3–8.0	359–882
Upper-mountain	0.40–0.46	0.54–0.60	0.12–0.13	3.3–3.7	364–404
High mountain	0.55–0.91	0.09–0.45	0.07–0.14	4.4–22.7	488–2498

Foot-note: The convention meanings see in **Table 4**.

5. Prognoses and paleo-reconstructions for landscape-zonal systems of the Volga River basin

5.1 Methods of predictive mapping

Ideologically, prognostic landscape-zonal mapping was based on the fundamental concept of global ecology concerning the close relationship between natural zonality and the heat-to-moisture ratio^[28,29], which was characterized through the Vysotsky–Ivanov’s annual humidity factor (F_{hum}). In the Volga River basin, regional phytocoenological units show a fairly strong dependence on this coefficient (see above **Table 2**). Moreover, statistical analysis revealed highly significant correlations between positions of zonal (sub-zonal) boundaries and F_{hum} (see below). These correlations were used for making a prognostic map of natural zones (sub-zones) in the region based on corresponding F_{hum} maps^[9].

These relationships formed the basis of predictive and paleogeographic mapping of regional bioclimatic conditions in the Volga River basin. The compilation of forecast maps using the GISS-1993 model was accompanied by the creation of analytical models of landscape-ecological transitions based on the method described above. The models took into account the partial mean-weighted effect of temperatures and precipitation (for the cold and warm periods of the year individually) on the behavior of zonal ecosystems. The set of such transitions significantly refines the overall pattern of change in the structure of the natural zoning of a region depicted in the forecast maps. The resulting landscape-geophysical relationships ensure quite effective use of the actualism method in numerical ecological forecasting and reconstruction of the landscape-ecological past.

The initial, pre-prognostic step of the work consisted in the determination of base (contemporary)

hydro-climatic conditions of the region. Two independent algorithms, cartographic and analytical, were used in prognostic modeling. Both types of models were developed on a much larger scale than it had been done before (1:2,500,000). With this purpose, a mathematical-cartographic analysis of structure-function connections in the regional systems has been carried out with the use of maps from the Atlas presented in the work^[9]. The known information-statistical methods^[46] were used to obtain matrices of partial coefficients of connections of phytocoenological and soil units with the main hydrothermal parameters: the mean January and July temperatures, precipitation total (annual, of the cold and warm seasons), annual values of evapotranspiration and runoff (surface and subsurface), and different coefficients of humidification, etc. Each matrix of partial connections forms a system of climatic niches of the objects under consideration. An individual column (vector) describes the ecological niche of a certain gradation of the phenomenon in the space of values of a certain factor. These matrices were used to obtain taxonomic base norms of the above hydrothermal parameters—the values average weighed by the territory.

Base values of F_{hum} were taken (with an interval of 25 km) on the boundaries of natural zones and subzones and processed statistically. Each boundary included 95 to 280 points. For most boundaries, the distribution of F_{hum} turned out very distant from the norm, with marked negative excesses, therefore, we had to divide each of the excerpts into two or three sub-excerpts according to the longitude-sector division of the zonal or sub-zonal boundary. The coefficient of variation of parameter F_{hum} in each of the combinations obtained did not exceed 4%–6%, and only for the boundaries of forest-steppe and steppe zones it was 10%–11%. As a whole, this is evidence

of the high significance of the obtained spatial connections of zonal and sub-zonal boundaries with the index of annual warmth to humidity ratio. These connections were further used for paleogeographical mapping of the system of natural zones of the region, on the basis of the corresponding maps of coefficient of humidification.

In contrast to rather schematic data on the global system of landscape-geophysical connections^[47], as well as analogous scanty information on the Russian Plain^[35], the stricter and more statistically substantiated regularities of the distribution of coefficient of humidification over natural zones (subzones) have been obtained for the territory of the Volga River basin, with two longitude-sector

versions (**Table 6**). Extreme values of each F_{hum} interval fall on the southern and northern boundaries of the corresponding natural zone or subzone. Quite significant were the intra-zonal longitude-sector changes in the warmth to humidity ratios determined by climate continentality. The greater continentality corresponded to the lower F_{hum} value, which conformed to the boundary conditions of a given natural zone (subzone). Even within the boundaries of the Russian Plain, the same zonal subdivision in the eastern, more continental sector is distinguished by higher aridity, and this longitudinal shift of relative humidity is comparable to the shift of zonal boundaries southwards for a whole subzone.

Table 6. Comparison of zonal-regional atmospheric humidity factors F_{hum} for territory of Volga River basin with the same coefficients which reflect the natural zonality of Russian Plain and the planetary system of zonality as well

Nature zones (subzones)	World system of nature zones, by Volobuev ^[47]	Russian Plain, by Isachenko ^[35]	Volga River basin and its encirclement	
			West sector	East sector
Middle taiga	1.87–2.00	1.07–1.76	>1.88	>1.62
South taiga	1.52–1.61	1.33–1.69	1.63–1.88	1.35–1.62
Mixed forest	1.20–1.24	0.78–1.46	1.22–1.63	1.00–1.35
Broadleaf forests	0.99–1.03	1.08–1.18	1.09–1.22	0.97–1.00
Typical and south forest-steppe	0.73–0.74	0.67–0.98	0.76–1.09	0.76–0.97
North steppe		0.51–0.80	0.70–0.90	0.60–0.76

*) Data are showed for the boundaries between nature zones and sub-zones.

In parallel, analytical models of predictive landscape-ecological transitions and paleogeographic deviations were created by the methods described above. The procedure of analytical prognosis involved (1) ordination of zonal vegetation units along the gradients of baseline climatic parameters and (2) quantitative assessment of the most probable transformations of these units under the effect of climatic changes expected within the period of interest. In particular, the most probable degrees of deviation from the baseline functional state by the years 2050, 2075, 2100, and Mikulino optimum were calculated for forest formations and landscape-zonal systems. In these models, the weighted-mean influence of changes in temperature and precipitation (for the warm and cold seasons separately) on the behavior of ecosystems was taken into account. The multitude of landscape-ecological transitions revealed in this

way added important details to the general picture of changes in the structure of natural zonality shown in the prognostic and paleogeographic maps of the Volga River region.

All paleo-prognostic landscape-zonal constructions are based on a rather close regional connection of plant formations with the annual humidity factor (see **Table 2**). Climatic niches of vegetation form a single continued series by this factor, without any marked leaps and with continuously changing taxonomic norms of F_{hum} . Such series points to a sequence of anticipated phytocoenological transitions at this or that climatic trend. For example, at a decrease in F_{hum} from 1.85–1.65 to 1.23–1.12, the firwoods of middle and south taiga of the Upper Volga must transform into broad-leaved dark-coniferous and/or pine formations, and then the latter—into the more continental dark-coniferous sub-taiga of the

lower Kama River and into broad-leaved and pine forests.

Summer moisture content in soil also correlates well with the coefficient of humidification, determining the latitude-zonal character of its distribution both at present and in the future. For agro-phytocoenoses of the Volga River basin, the connection between the July resources of productive moisture in a 1-m soil layer ($W-100$) and the parameter F_{hum} is as follows:

$$(W-100) = 98.57 \cdot F_{hum} - 19.8; R = 0.86; R^2 = 0.73 \quad (16)$$

The calculations of hydrothermal conditions of the above epochs of the geological past were based on the materials of point paleo-climatic reconstructions (by separate profiles) for the territory of the Russian Plain, according to Gerasimov and Velichko^[48], Velichko *et al.*^[49], Velichko and Klimanov^[50]. Unfortunately, the network of base points proved to be insufficient for standard mapping on the given scale. The way out was found as follows. First, based on the idea of a single character of plant cover evolution in the Volga River basin in Holocene^[51], one might assume the territorial integrity of bioclimatic conditions of the region at all stages of development of its contemporary zonal structure. Second, following the developments^[49], we have accepted that the total character of the main hydrothermal fields of the region in the geological epochs under consideration was analogous to the modern one. Consequently, the pattern of relative differences between some or other regions was similar. This allowed a nonlinear extrapolation to map sites lacking factual data, using the maps of hydrothermal parameters for the base period as analogies.

5.2 Main features of climate forecast

Regional landscape-ecological calculations and mapping were carried out according to Goddard's GISS-1993 mode, based on the original global model GISS-1988^[52]. For the forest-steppe and steppe zones of the Russian Plain, the deviations of the calculated values from the actual ones (when simulating the modern climate) are: according to the average

temperature of January and July, respectively, -4 , $(+2)^0$ and -1 , $(+1)^0$. These figures are much lower than those, which is given by two other models—GFDL and UKMO^[44]. According to the GISS-1993 model, we can judge the ecological situation with an increase in global temperature in the coming decades no more than 1.5^0 , the achievement of the goal of which is provided for by the Paris Agreement (2015) on climate change.

According to the GISS-1993 model, the mean global temperature in the forecast periods of up to 2050, 2075, and 2100 is anticipated to increase due to anthropogenic impact for $0.8-1.0^0$, $2.0-2.2^0$, and $3.0-4.0^0$, respectively, as compared with the base level (**Table 7**). This prognosis has already been partially justified: in 1995–1999, which turned out to be the warmest of instrumentally monitored periods, the deviation of mean annual temperature from the 20-year norm of the “pre-industrial period” (1886–1905) on the European territory of Russia was $0.7-0.8^0$ to 1.9^0 ^[53]. The GISS model shows also that in the Middle belt of the Russian Plain during the first (70-year) forecast period the greater temperature increase is expected not in the cold but in the warm season. It is of great eco-logical significance because, as we have already shown before, the structural changes in vegetation and soils are determined mostly by their functional shifts just in the period of vegetation.

By 2050, the mean July temperature in the overwhelming majority of landscapes of the Volga River basin will grow to $1.1-1.3^0$, and in the sub-taiga zone and in the zone of broad-leaved forests—for $1.5-1.7^0$ here and there (see **Table 7**). At the same time, the mean January temperature will grow much less, mainly for 0^0 to $0.2-0.5^0$ (in the Upper Volga Region to 1.4^0), and on the territories of mixed and broad-leaved forests and forest-steppe, the winter temperature might even decrease for $0.2-0.8^0$. Such thermal trend will cause an inevitable growth of climate continentality, with the corresponding enhancement of probability of extreme meteorological situations, which should increase the instability of function of geo(eco)systems and, accordingly, speed up their structural transformations.

Table 7. Basic taxonomic norms of climatic parameters in the Volga River basin and their predicted deviations, by the GISS-1993 model

Types and subtypes of formation	Formation groups	Average t_{Jun} , °C			Average t_{July} , °C			Annual precipitation, mm		
		Base	2050	2100	Base	2050	2100	Base	2050	2100
Dark-coniferous middle and southern taiga and subtaiga forests		-12.2	0.6	3.7	16.0	1.3	3.2	768	14	172
		-15.6	1.4	5.0	16.7	1.1	3.0	697	122	250
		-11.6	0.5	4.0	17.2	0.8	2.7	759	94	229
		-11.9	0.6	3.9	17.4	0.7	2.7	737	59	193
		-10.2	0.2	3.3	17.3	0.7	3.0	763	62	196
		-14.7	0.9	4.8	18.0	0.8	2.6	679	54	170
		-13.9	0.5	4.5	18.6	0.8	2.6	630	44	158
Pine and broadleaf-pine taiga and subtaiga forests		-12.2	0.5	4.1	18.8	1.1	2.8	650	56	148
		-12.0	0.3	3.8	19.2	1.1	2.8	652	50	178
		-11.0	0.1	3.7	18.7	1.0	3.0	655	64	156
Broadleaf forests		-11.5	-0.2	3.3	19.6	1.1	3.0	602	56	134
		-12.5	0.3	4.3	20.2	1.0	3.0	556	81	121
Typical and southern forest-steppe		-11.1	0.1	3.5	20.5	1.3	3.3	536	109	158
		-12.3	0.4	3.9	21.6	0.9	3.0	507	77	126
Steppe		-14.9	0.9	4.6	20.9	0.9	2.7	509	48	81
		-14.3	0.4	4.4	22.0	0.8	2.9	438	66	81

The rate of warming between 2050 and 2075 will remain generally the same, with the monthly average temperatures exceeding the corresponding baseline values by 2.2–2.3°. Finally, by 2100, the general increase in the average January temperature (up to 4.5–5.0°) will become a priority. Thus, considerable shifts in the thermal energy supply to ecosystems will take place in all natural zones of the Volga River basin, with the ecological effect of these shifts increasing in a north-south direction. Boreal and nemoral forests will remain under climatic conditions of the temperate belt. Formations of the southern forest steppe and, especially, the northern steppe will pass from the sub-boreal to the subtropical thermal-radiation category according to the Volobuev's classification^[54], i.e., they will be in a different climatic belt.

The anthropogenic warming will be accom-

panied by a general increase in precipitation. By 2050 and 2100, the annual amounts of precipitation in the middle and southern taiga subzone will increase by 11–120 and 200–270 mm, and those in the forest-steppe with broadleaf forests and in the northern steppe will increase by 60–80 and 100–150 mm, respectively. In percentage, the difference will show up only in the end of the forecast period: for the time interval of 2010–2050, the annual precipitation growth will be 9%–18% → 26%–37% in the first case and 9%–13% → 18%–26% in the second case. It is important to emphasize that it will occur mainly (for 70%–80% and more) due to the increment of precipitation in the warm season.

5.3 Prognostic and paleogeographic scenarios of zonal structure of the basin territory

According to the models obtained, the following equifinal transformations of the zonal structure

of the boreal and sub-boreal belts of the Russian Plain have been predicted (Figures 2, 4(a), and 5).

(1) The rise of temperature will not be effectively counterbalanced by the increase in precipitation caused by global warming. Therefore, it is expected that the annual atmospheric humidity factor and productive soil moisture content in summer will decrease throughout the region (see Table 7); thus, a

growing thermo-arid bioclimatic trend will be observed. By the year 2050, F_{hum} in virtually all middle and southern taiga ecosystems will decrease by 0.1–0.2, and the soil moisture content in July will become 20%–30% lower. This will create conditions for the transgression of mixed forest formations and then oak forests from the south, as was the case, for example, in the xero-thermal period of the Holocene.

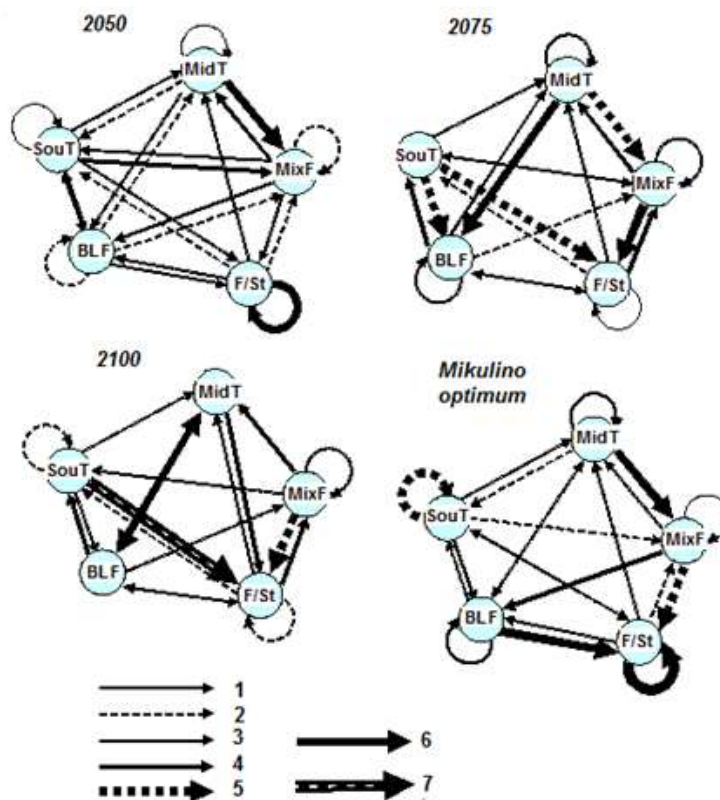


Figure 5. Directions and probabilities of functional transformation and deviations of the landscape-zonal systems on the territory of the Volga River basin and its surrounding for different prognostic dates, according to GISS model, and for paleoreconstruction for Mikulino (Eemian) interglacial optimum. Landscape-zonal systems: Mid T—middle taiga; Sou T—southern taiga; Mix F—mixed forest; BL F—broadleaf forest; F/St—typical and southern forest-steppe. Probabilities of landscape-zonal transitions and deviations: 1—0.10 and less; 2—0.11–0.20; 3—0.21–0.30; 4—0.31–0.40; 5—0.41–0.50; 6—0.51–0.60; 7—0.81–0.90.

Sub-taiga pine and linden-oak forests will also become unstable, giving way to mixed herb-grass pine forests characteristic of the typical forest-steppe. Finally, a significant decrease in moisture supply at the initial stage ($\Delta F_{hum} = -0.11$) will entail further aridization of the northern steppe in the Trans-Volga region near Samara.

(2) Two zonal types of the natural environment will receive the greatest territorial development: on the one hand, mixed forests (with both dark coniferous species and pine stands predominant); on the other hand, typical and southern forest-steppe. Meanwhile, already at the forecast stage for 2050–

2075, the forest-steppe zone will have priority, which will become the dominant absorbing object (absorbent) at the end of the forecast period 2050–2075. As a result, by the middle of the 22nd century, almost the entire territory of the main catchment area of the Volga River basin will be in sub-boreal bioclimatic conditions.

(3) In the eastern sector of the taiga zone, however, a weak thermo-humid trend will manifest itself ($\Delta F_{hum} = 0.07–0.08$), and southern taiga formations will gradually acquire the state characteristic of their western, less continental counterparts. Strong manifestations of the thermo-arid trend in the southern

taiga of the Upper Volga Region ($\Delta F_{\text{hum}} = -0.34$) will attenuate bioclimatic contrasts between longitudinal sectors throughout the taiga zone. Aridization will also spread to the typical and southern forest-steppe sub-zones. In this situation ($\Delta F_{\text{hum}} = -0.38$), mixed herb-grass oak forests will be most vulnerable, being gradually displaced by the southern forest-steppe expanding from the Cisural Region.

(4) Two zonal types of the natural environment will receive the greatest territorial development: on the one hand, mixed forests (with both dark coniferous species and pine stands predominant); on the other hand, typical and southern forest-steppe. Meanwhile, already at the forecast stage for 2050–2075, the forest-steppe zone will have priority, which will become the dominant absorbing object (absorbent) at the end of the forecast period 2050–2075. As a result, by the middle of the 22nd century, almost the entire territory of the main catchment area of the Volga River basin will be in sub-boreal bioclimatic conditions.

(5) The nemoral forest sub-zone will completely change its location, going beyond the bounds of the Central Russian and Volga highlands. The territory of modern deciduous forests will be completely absorbed by middle forest-steppe formations, which will partially occupy even the Cis-Ural sub-taiga. The nemoral forest communities will show active transgression, first in the southern and then in the middle taiga, creating new mixed phytocoenological structures and thus expanding the total area of the sub-taiga zone.

(6) At the third stage (2075–2100), aridization will become less active, especially in mixed forests of the eastern sector and in steppe pine and oak forests. However, it will still progress in the western sector, mainly in middle taiga fir-spruce forests and in mixed and broadleaf forests (see **Figures 4(a)** and **2(b)**). Thus, the thermo-arid trend will be initially manifested mainly in the eastern sector of the Volga River basin; by the year 2100, however, its effect will be stronger in the western sector.

This, the hot-arid bioclimatic trend should disrupt the stability of forest formations on the Russian Plain in the entire forest-steppe transition zone. In general, the progressive encroachment of the steppe

onto the forest is expected in the entire 100–200 km (along with the meridian) space in the south of the forest zone. Such a landscape-ecological forecast is very unfavorable for forestry and will inevitably aggravate the problem of forest and, in addition, water resource conservation.

(7) The above landscape-ecological prognosis is in good agreement with global scenarios of natural zonality that are based on different models, including the GISS model, and envisage a twofold increase in the atmospheric CO₂ concentration^[55,56], i.e., the situation expected in 2100. The maps made by the authors of these scenarios show that forest-steppe and steppe formations will deeply penetrate the forest zone of Eurasia. In European Russia, they will probably expand mainly over the Central Russian and Volga uplands. A prognosis made for the territory of the former Soviet Union^[6] is fairly similar to the results obtained with our model.

The constructed maps and analytical models of zonal deviations from the base period into two paleogeographic sections: the optima of the Mikulino (Eemian) interglacial and the Holocene (Figures 3 and 5), revealed an inverse hot-arid trend, i.e., a retrospective manifestation of the same trend predicted for the given bioclimatic trend, but with the opposite sign. It was proved that the parameter F_{hum} rather than simple temperature similarity, as practiced earlier^[4,49], gives grounds to consider the optima of the Mikulino interglacial and Holocene as paleo-analogs of predicted environmental situations. It was also established that the well-known paleogeographic constructions at the optimum of the Mikulino interglacial^[49] are debatable. Within the boreal belt, the initial paleoclimatic data have already initially predetermined the hot-arid type of deviations of the climate conditions of the Mikulino optimum from the current climate.

6. Mountain and piedmont landscape systems of the Northern Macroslope of the Greater Caucasus

6.1 Introductory notes

Conservation of the biodiversity and natural resources of mountain ecosystems is an important task.

Natural associations of mountains are among the most dynamic units of the biosphere; they are highly sensitive to both climatic changes and anthropogenic impacts. Climatic variations cause shifts in the heat and moisture supply to the alpine stratum, which results in periodic destabilization of mountain slopes and consequent catastrophic phenomena, such as landslides, mudflows, and avalanches. They also play a role in the rearrangement of the alpine phyto-biota, including a shift of the upper timberline, an important biogeographic and landscape boundary in high mountains. Here, the author describes the experience in predicting the possible ecological consequences of global climate warming for regional landscapes of the Northern macro-slope of Great Caucasus. The landscape ecological approach implies revealing the spatial diversity of climate-related changes in landscapes determined by their macro-catenic organization under different conditions of vertical zonality. The landscape ecological prediction itself consists of two stages, analytical and cartographic, which are considered below.

6.2 Regional climatic prediction

For mountainous areas, the prediction stage of analysis consists primarily in establishing spatial relationships between climatic parameters (temperatures and precipitation) and morphometric quantities (MQ) of mountainous terrain. Let us give an example with the northern macro slope of the Greater Caucasus^[45].

The predicted changes in the mean January temperature are determined by three predictors: watershed area, true altitude, and basic temperature. The latter two factors also determine the change in the mean July temperature.

The results of climate prediction mapping following the NASA model and our model have been compared. The spatial structure of our model is incommensurably more complex and contrasting. It is characterized by the high level of significance ($P < 10^{-4}$ for 2050 and $P < 10^{-3}$ for 2100).

At the first stage, we calculated the matrices of

the basic climatic parameters (temperature and precipitation) from the data of the hydro-meteorological network on the northern macro-slope of the Greater Caucasus. For this purpose, we performed a statistical analysis of the relationships of climatic parameters with the absolute elevation (a.s.l.) and 17 characteristics of MQ. The original matrix of the topography was based on NASA satellite data on the Greater Caucasus (SRTM30) with a resolution of 30 angular minutes. It was transformed into intermediate Kavraisky's projection with a grid step of 500 m. The Analytical GIS Eco software^[57] was used for determining statistical relationships, calculating the matrices of the basic climatic parameters, and drawing detailed climatic maps.

At the second stage, we calculated the matrices of changes in climatic parameters for two prognostic years: 2050 and 2100. Preliminary, E GISS model data were transformed to a 10×10 grid using the Delaunay triangulation. After that, the parameters were interpolated based on their statistical relationships with the topography of the Greater Caucasus found earlier, as well as basic climatic parameters.

The regional scenario of anthropogenic climatic changes in the ongoing century was taken from the latest global prognostic climatic GISS Model E belonging to the family of models of general atmospheric circulation^[41]. The regression equations characterize the statistical connections between the climate and the mountain relief of the Greater Caucasus (**Table 8**). Here, the first three members are the key MQ predictors of spatial climate variability. The mean January (t_{Jan}) and July (t_{July}) temperatures are quite closely associated with the relief characteristics ($P < 10^{-6}$, $r_S = 0.96$ and 0.72). The basic spatial changes of t_{Jan} and t_{July} depend on the true altitude by 74% and 87%, respectively. In the former case, there is also the dependence on the slope angle (by 15%) and the intensity of southern illumination of slopes (by 12%). The July temperature is additionally associated with the average convexity of relief forms (by 8%) and concavity of the profile of slopes (by 5%).

Table 8. Statistic connections of base and predictive (by global E GISS model) to climate parameters of Great Caucasus with relief

Climate parameter		Equations of multiple regression	<i>r_s</i>	<i>P</i>
Average temperature	January	$X = [-73.5 \cdot Z + 14.5 \cdot GA + 12.0 \cdot F(35^0, 180^0)] \cdot 0.249 - 2.8$	0.72	$<10^{-6}$
	July	$X = (-87.3 \cdot Z + 7.9 \cdot H - 4.8 \cdot kv) \cdot 0.277 + 23.6$	0.96	$<10^{-6}$
Precipitation amount of cold period (at regions)	West	$X = (-45 \cdot F(35^0, 140^0) + 27.8 \cdot GA - 27.2 \cdot Z) \cdot 12.704 + 569.2$	0.57	$<10^{-3}$
	Central	$X = [70.4 \cdot Z + 26.7 \cdot MCA + 2.9 \cdot F(35^0, 325^0)] \cdot 8.236 - 85.4$	0.77	$<10^{-6}$
	East	$X = (-53.5 \cdot kv - 39.4 \cdot MCA - 7.1 \cdot M) \cdot 9.591 + 655.2$	0.76	$<10^{-4}$
Precipitation amount of warm period (at regions)	West	$X = (-60.3 \cdot kh + 32.8 \cdot GA + 6.9 \cdot MCA) \cdot 9.761 + 904.8$	0.49	$<10^{-2}$
	Central	$X = (79.7 \cdot Z - 10.6 \cdot kh + 9.7 \cdot MCA) \cdot 5.553 + 461.3$	0.75	$<10^{-6}$
	East	$X = (-41.1 \cdot F(35^0, 270^0) + 34.1 \cdot Z - 24.8 \cdot MCA) \cdot 8.299 + 675.9$	0.70	$<10^{-4}$
Change of average temperature to year 2050	January	$X = (-36.0 \cdot MCA - 35.1 \cdot Z - 28.9 \cdot t_{jan}) \cdot 0.011 + 1.7$	0.62	$<10^{-4}$
	July	$X = (-49.6 \cdot t_{july} - 48.6 \cdot Z + 1.8 \cdot k_{max}) \cdot 0.408 + 20.8$	0.60	$<10^{-3}$
Change of precipitation amount to year 2050	Cold period	$X = (-42.8 \cdot Z - 35.8 \cdot MCA - 21.4 \cdot t_{jan}) \cdot 0.015 + 2.2$	0.57	$<10^{-3}$
	Warm period	$X = (-50.1 \cdot t_{july} - 48.9 \cdot Z - 1.0 \cdot GA) \cdot 0.274 + 14.7$	0.65	$<10^{-4}$
Change of average temperature to year 2100	January	$X = (-55.2 \cdot r_{cp} - 43.2 \cdot H + 1.6 \cdot Z) \cdot 0.704 + 24.2$	0.56	$<10^{-3}$
	July	$X = (59.4 \cdot H - 37.0 \cdot kv - 3.6 \cdot r_{wp}) \cdot 0.648 + 19.8$	0.56	$<10^{-3}$
Change of precipitation amount to year 2100	Cold period	$X = (-37.1 \cdot H - 36.1 \cdot r_{ann} - 26.8 \cdot MCA) \cdot 0.573 + 19.3$	0.56	$<10^{-3}$

Foot-note: Average temperature; t_{jan} —for January and t_{july} —for July. Total precipitation: r_{cp} —for the cold period and r_{wp} —for the warm period. Z is true altitude. MCA is watershed area. GA is the slope angle. The curvature: H , the average; k_{max} , the maximum; kv , the vertical, kh , the horizontal. $F(35^0, 145^0)$ is intensity of illumination of slopes (solar declination and azimuth are given in parentheses). The regression coefficients before the morphometric values are expressed in percentage terms corresponding to their relative contribution to spatial variability of the climate parameter. Statistical characteristics: r_s —the Spearman's correlation; P —the level of significance.

6.3. Regional analytic predictive-ecological model

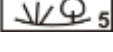
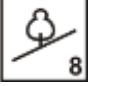
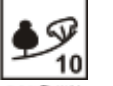
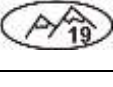
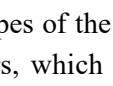
Groups of landscapes of the Northern macro-slope of the Greater Caucasus (Table 9) were considered as regional objects of environmental forecasting. First of all, one should note multiple transitions of nearly all landscape groups (LG) not only into the mountain landscapes in adjacent altitudinal layers but also into quite distant natural complexes: right up to the plain-hilly piedmonts. At the same time, the respective transitions of hydrothermal states of landscapes are inevitable: from cold to warm-temperate and from humid and semi-humid to semiarid. Such complexity of the system of anticipated landscape transformations is because each LG combines regional natural complexes occurring under different geomorphological conditions: on mountain ridges and flat watersheds, on the slopes with different circulation and solar exposure in intermountain valleys and hollows. Hence, quite a lot of functional and structural transitions with rather low values of dominant transition probabilities ($P_{ij} \leq 0.20$) appear in each landscape group in response to the same climatic signal.

Landscapes with the minimum stability ($P_{ii} \leq$

0.50) occur in all altitudinal layers, except for the high mountain layer. These are piedmont steppes and meadow steppes (landscape group 4), the lower- and middle-mountain oak and hornbeam-beech forests, as well as meadow-steppe and shrubs spreading in their place (landscape groups 6, 8, and 11), and finally the upper-mountain pine and birch forests (LG 15). Comparatively high stability ($P_{ii} \geq 0.59$) is typical of the lower- and upper-mountain broadleaf and mixed forests (LG 7 and LG 13), as well as mountain-hollow semiarid steppes (LG 12). The highest stability ($P_{ij} \geq 0.85-0.90$) is characteristic of landscapes of the sub-nival and nival-glacial zones.

In the first interval (1990–2050), the velocities of landscape transitions in most cases will be much higher than in the second interval (2050–2100). It seems that the functional and structural landscape transformations in the second half of the 21st century will slow down, especially in foothills and low mountains. Both forecast periods are characterized by a common tendency: the intensity of landscape transitions weakens (parameter m_{ij} decreases from 0.20–0.26 to 0.04–0.08) in proportion to ascending the mountains, with simultaneous thinning out of the network of transitions.

Table 9. Landscapes of the northern macroslope of the Greater Caucasus (Central and partially West), according to classification by Beruchashvili *et al.*^[52]

Landscape type	Landscape subtype	Landscape groups (LG)	
		Serial number and name	Symbol
Plain warm-temperate semi-humid	Meadow-steppe and shrubby	1. Plain-hilly, with meadow-steppes and shrubs	
	Plain warm-temperate and temperate semiarid	Steppe	2. Plain-hilly, with forb- and vermouth-grass steppes
3. Plain-hilly intermontane, with forb-grass meadow-steppes			
4. Foothilly plain-hilly, with steppes, meadow-steppes, and shrubs			
Plain sub-hydromorphic	Valley mire solonchak, meadow	5. Low-land accumulative and flood plain, with meadows and forests, more rarely with solonetz and solonchaks	
Mountain temperate humid	Low- and middle-mountain forest	6. Middle-mountain, with oak and horn-beam-beech forests and post-forest meadows	
	Low-mountain forest	7. Low-mountain, with oak and hornbeam-beech forests and meadows	
	Middle-mountain forest	8. Middle-mountain karst, with beech forests	
9. Low-mountain karst, with hornbeam-beech forests, post-forest meadows and shrubs			
Mountain temperate semi-humid	Mountain-hollow forest and steppe	10. Mountain-hollow, with oak forests, steppes, shrubs, shibliak and frigana, and light forests	
	Low-middle mountain forest, meadow and steppe	11. Low- and middle-mountain, with steppes, shrubs, meadow-steppes, more rarely with beech and hornbeam-oak forests	
Mountain temperate semi-arid	Mountain-hollow steppe	12. Mountain-hollow, with mountain-steppe, shrubby, shibliak and frigana vegetation	
Mountain cold-temperate semi-humid and semi-arid	High-mountain pine and birch	13. Middle-mountain, with beech/dark-coniferous forests	
		14. High-mountain erosion-denudation and paleo-glacial, with pine and birch forests	
		15. high-mountain, with pine, more rarely birch forests	
High-mountain cold meadow	High-mountain subalpine forest-shrub-meadow	16. High-mountain, with meadows, shrubs and light forests	
	High-mountain alpine shrub-meadow	17. High-mountain, with alpine meadows	
	High-mountain subnival	18. High-mountain subnival	
		19. Glaciers, highland deserts	

In the or-graph (**Figure 6**), the arrows of transitions are directed mainly downward along the macro-slope of the Greater Caucasus. It means that landscape transformations in each altitudinal layer

will proceed mainly toward landscapes of the lower warmer and more humidified layers, which corresponds to the general thermo-arid climatic trend. Accordingly, landscape boundaries will also shift

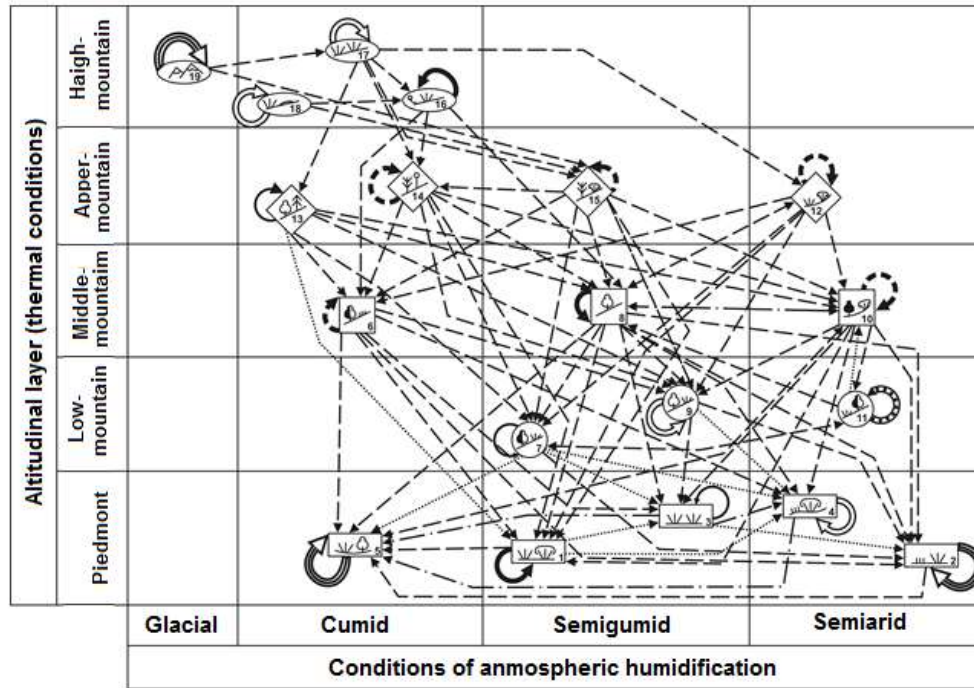


Figure 6. The northern macro-slope of the Greater Caucasus. The or-graphs of functional landscape-ecological transitions for 2050, in accordance with the E GISS climate prediction model, between the landscape groups (see **Table 9**) located at different altitudinal layers under different conditions of atmospheric humidification.

upward along the slopes.

In the high-mountain layer, alpine meadows (LG 17) will undergo the most substantial transformation. They will partially pass into the state of upper-mountain birch-pine forests (LG 15; $P_{ij} = 0.22$, $m_{ij} = 0.056$) on ridge slopes and into mountain-hollow semiarid shrub steppes (LG 12; $P_{ij} = 0.17$, $m_{ij} = 0.043$) in intermountain depressions. Subalpine meadows and light forests (LG 16, $m_{ij} = 0.047$) will transgress here as well. The subalpine communities will begin to pass into the neighboring upper-mountain ecosystems: humid beech/dark-coniferous forests in the West Caucasus (LG 13; $m_{ij} = 0.054$) and into semiarid birch/pine forests to the east from the Elbrus (LG 14; $m_{ij} = 0.071$). They will also be possibly transformed into middle-mountain beech forests (LG 8; $m_{ij} = 0.047$). It will amount to about 40% of the total transformations of subalpine ecosystems.

Both middle-mountain forests and forest-meadow-steppe complexes of intermountain hollows (LG 6, 8, and 10; $m_{ij} = 0.065-0.100$) will spread into the upper-mountain layer (LG 13, 14, and 15). In the Kuban River basin, dark-coniferous trees will be displaced by beeches and hornbeams, and the landscapes here will appear as humid forest middle-mountains (LG 6 and 8). A real steppification of

upper-mountain forests will begin in the Central Caucasus, right up to the state of piedmont forb-grass and vermouth-bunch-grass steppes (LG 2; $m_{ij} = 0.049-0.043$).

In the middle mountains, broadleaf forests (LG 6) will be transformed by nearly 30% into their low-mountain analogs (LG 7 and 9; $m_{ij} = 0.073-0.078$), while post forest meadows will even get the appearance of piedmont meadow steppes (LG 1). Finally, the prairiefication and steppification processes will involve the entire low-mountain layer. Its humid oak and hornbeam-beech forests will be transformed simultaneously in several directions, with final transformation into forb-grass meadow steppes and steppes (LG 1 and 3).

Stabilization probabilities P_{ii} and mutual transitions P_{ij} : 1—0.01–0.10; 2—0.11–0.20; 3—0.21–0.30; 4—0.31–0.40; 5—0.41–0.50; 6—0.51–0.60; 7—0.61–0.70; 8—0.71–0.80; 9—0.81–0.90; 10—0.91–1.00.

6.4 Regional landscape-ecological prognosis in cartographical expression

Regional predictive mapping was carried out also to help the operation with ecological niches. At the same time, it was considered only thermal niches

as the most significant. The quantitative approaches to prognostic ecological and geobotanical mapping recently developed abroad^[58] are intended for drawing large-scale maps. However, these approaches have never been used for drawing prediction maps on a time scale. Moreover, we do not know of any experience in using these methods for mapping the functional parameters of forest ecosystems in the framework of a global climatic scenario. In landscape ecological analysis, we use approaches based on *new geomorphometric methods*^[36,59,60] for drawing Spatio-temporal maps.

Geomorphometry is the science of quantitative description of terrain, which has been substantially developed during the past 50 years^[61], provides methods for obtaining the pattern of the spatial distribution of soil-biotic and hydrothermal parameters of geo(eco)systems. Multifold edificatory properties of the terrain make it possible to interpolate and extrapolate data measured (or calculated) in representative test grounds (which was justified in the course of analysis); this substantially extends the analyzed area. Earlier methods of quantitative description of terrain are restricted to the use of six basic morphometric parameters. We have introduced a system of 18 parameters, developed new geomorphological classification frameworks, and derived better algorithms for the calculation of morphometric characteristics^[59,62].

For the prognostic mapping procedure, we used both reductant and absorber $C(ai/bj)$ values for two climatic factors: t_{jan} and t_{july} . Climatic caused transformation of regional nature complexes is expressed at the map by the certain shift of landscape boundaries. It is need to spoke mainly about phytocoenological shifts as the most real ones. Vector of this shift is determined by the oriental graph of transitions between the landscape groups. It is characterized in general by the *focal transformation of geosystems*, which is the leading form of their climate-genic transformations. The set of absorbents for each reducer is determined by significant probabilities P_{ij} of landscape-ecological transitions for a given forecast period, beginning from the highest value of P_{ij} . However, the dimension of space displacement of phytocoenological and correspond-

dingly landscape boundaries is determined much more difficult.

The prognostic cartographic problem was solved using exhaustive search among the binary relationships between landscape groups presented in the oriented graph of their mutual transitions. Every time, we considered a dynamic pair of objects: the absorbed object A (the reductant) and the absorbing object B (the absorber). It was assumed that not only an adjacent object but also a relatively remote one (a second-order, third-order, etc., neighbor) may be absorbed. The object B whose absorbing activity towards object A was the highest was the first choice. Since the probability of the transition $P_{ij}(A \rightarrow B) < 1$, it was reasonable to assume that the transformations of object A would always be localized ("focal"). In other words, the $A \rightarrow B$ transition must occur in parts, beginning from fragments ai of areal A that are most predisposed to such transformation, proceeding from the basic climatic conditions. How can we determine such fragments?

As has been mentioned, the projection of the ecological niche of a given LG to the t_{jan} or t_{july} field is made up of the dominant and peripheral parts of the niche. Our previous analysis of the mechanisms of formation of landscape-zonal systems and their boundaries has shown^[9] that the system-forming and spatially differentiating influence of transit (including hydrothermal) factors drastically increase on the periphery of natural complexes. Consequently, landscapes in the positions of the "fuzzy" part of the niche must be most sensitive to climatic signals. Such fragments a_i of areal A will be least stable and begin to transform first and foremost.

In the given example (**Table 10**), subalpine landscape group 16 is considered as a reducer. For the forecast period of 2050, the primary fragments of these landscapes, which will begin to lose their previous subalpine aspect, will be those in the ranges of $t_{jan} = -5.2 \div (-9.0)^0$ and $t_{july} = 13.5 \div 16.0^0$.

It is also necessary to find out a group of landscapes playing the role of absorbent, as well as to determine the relative area absorbed by the latter from some or other reducer. It is accepted that the absorbent for each fragment a_i of the reduced (absorbed) areal A will be an adequate landscape group, where

the ecological dominant is in the same (or similar) temperature range as the absorbed fragment. The absorbent was searched by comparing the vectors of climatic niches of the reducer with the niches of all potential absorbents. In this case (see **Table 10**), there were two absorbents for t_{Jan} : (1) LG 13 for subalpine landscapes in the range of $-7.0 \div (-9.0)^0$ and (2) LG 14 for the landscapes in the range of $5.2 \div (-7.0)^0$. The predominant absorbent for t_{July} was revealed as well: it was the middle-mountain meadow-forest LG 8.

The absorbed area was assessed by the respective $C(a_i/b_j)$ value provided that the reduced fragment under consideration has been completely absorbed by the given forecast period. For example, proceeding from the data in **Table 10**, we accept that subalpine landscapes by 2050 will have reduced their areas by 12% and 24% in the mean January temperature transitions LG 16 \rightarrow LG 14 and LG 16 \rightarrow LG 13, respectively. For t_{July} , 15% of subalpine landscapes will pass into the state of middle-mountain beech forests (LG 8).

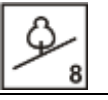
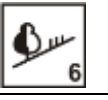
Later on, particular climatic maps were

superimposed on the landscape map (**Figure 6**). All fragments a_i of object A , adequate to object B by their state, which now became a part of areas of the absorbent or were included in its typological set, were found on this latter map. When moving to the next absorbent object C , i.e., analyzing the binary relation $A \rightarrow C$, we used the ordination of object A by the climatic factor that had not yet been considered. This operation was performed for all significant landscape-ecological transitions of object A into objects B, C, D , etc., in the order of diminution of parameter P_{ij} . When choosing the directions of absorption in the case of multiple equiprobable transitions, the preference was given to the nearest absorbent: the first-order neighbor.

The above algorithm was used to plot the landscape-ecological map of the northern slope of the Greater Caucasus for 2050 (**Figures 7 and 8**). The generalized representation of changes in the landscape mosaic of this region is given in **Table 11**. Values of $\sum \Delta S$ showed in brackets have been revealed in superposition process of average January and July

Table 10. The matrices of normalized partial coefficients of connection of subalpine forest-shrub-meadow landscapes (LG 16, reducer) and upper-mountain forest and middle-mountain forest-meadow natural complexes (LG 13, 14, 8, and 6, absorbents) with the mean January and July temperatures in 2050, according to the E GISS climate prediction model

Average January temperature	Landscape groups		
			
$-15.0 \div (-12.5)$	0.06		
$-12.5 \div (-10.5)$	0.23 +		0.03
$-10.5 \div (-9.0)$	0.29 •	0.30 +	0.24 +
$-9.0 \div (-7.0)$	0.24 +	0.36 •	0.30 •
$-7.0 \div (-5.2)$	0.12 +	0.27 +	0.34 •
$-5.2 \div (-4.0)$	0.05	0.07	0.08
$-4.0 \div (-3.0)$	0.01		0.02

Average July temperature	Landscape groups		
			
$0 \div 3.5$	0.06		
$3.5 \div 6.5$	0.05	0.04	
$6.5 \div 9.0$	0.13 •	0.09	
$9.0 \div 11.0$	0.24 •	0.10 •	
$11.0 \div 13.5$	0.32 +	0.32 +	0.01
$13.5 \div 16.0$	0.15 •	0.35 +	0.16 •
$16.0 \div 18.7$	0.04	0.08	0.62 +
$18.7 \div 21.0$			0.21 •

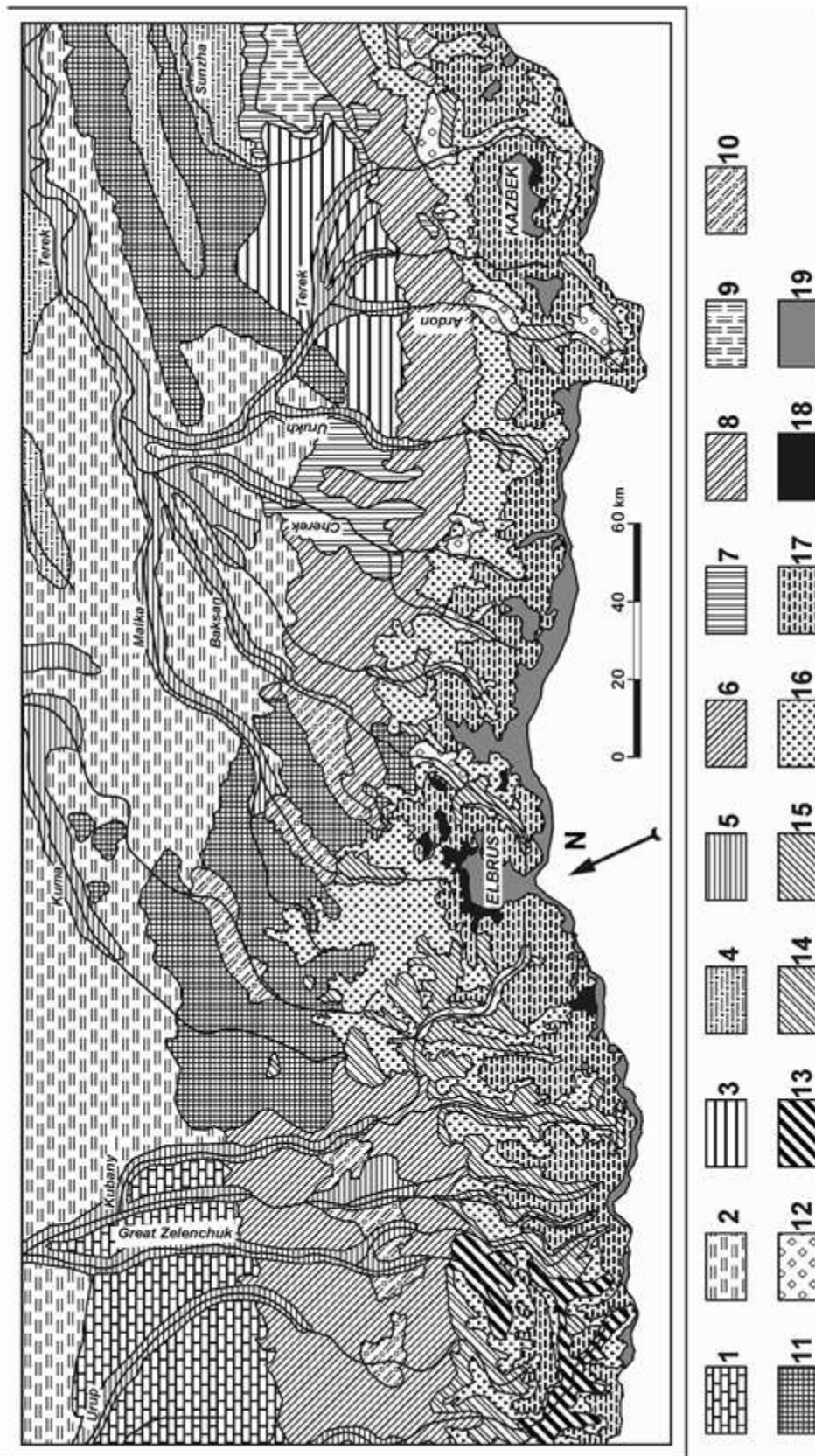


Figure 7. The fragment of landscape map of the northern macro-slope of the Greater Caucasus, according to Beruchashvili *et al.*^[52]. 1–19, landscape groups (see Table 9).

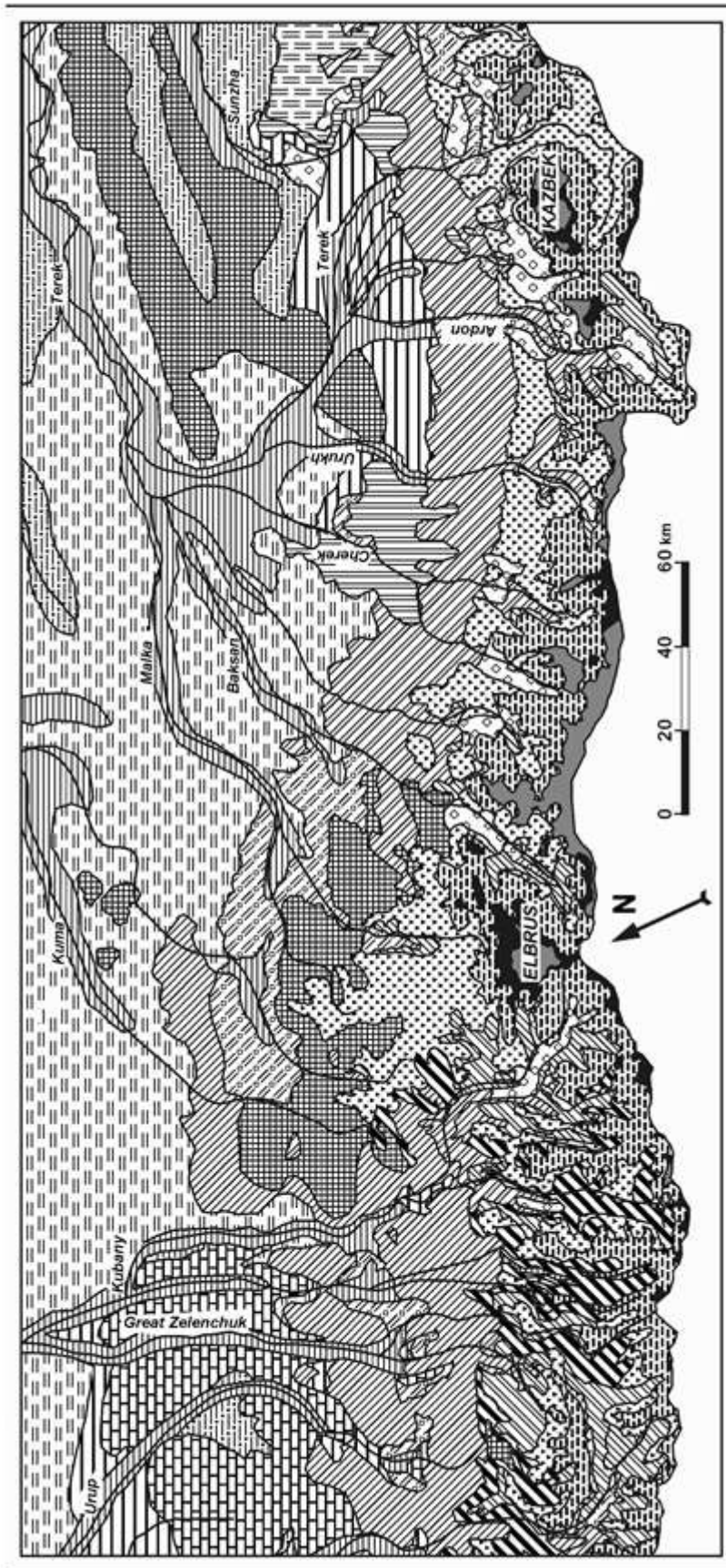
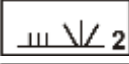
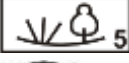
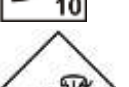
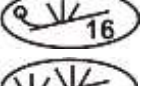
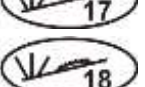
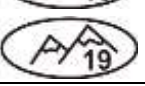


Figure 8. The map of landscape-ecological conditions of the northern macro-slope of the Greater Caucasus predicted for 2050 in accordance with the E GISS global climatic model. Map has been created by L.S. Sharaya. The symbols of landscape groups are the same as in **Figure 7** and **Table 9**.

Table 11. The northern macroslope of the Greater Caucasus. Relative changes in the areas of landscape groups as a result of their mutual transitions for 2050, according to the E GISS climate prediction model

High layers	Landscape groups	Changes of an area, ΔS		
		Gain + ΔS	Loss - ΔS	Result $\sum \Delta S$ *)
Piedmont		0.24	0.19	+0.05 (-0.01)
		0.05	0.39	-0.34 (+0.02)
		0.49	0.58	-0.09 (+0.21)
		0.59	0.29	+0.30 (+0.21)
		0.52	0.33	+0.19 (+0.12)
Low-mountain		0.74	0.54	+ 0.20 (- 0.16)
		0.81	0.52	+0.29 (+0.48)
		0.11	0.38	-0.27 (-0.21)
Middle-mountain		0.25	0.28	-0.03 (+0.09)
		0.40	0.30	+0.10 (+0.14)
		1.54	0.45	+1.09 (+0.54)
Upper-mountain		8.30	0.36	+7.94 (+0.69)
		0.52	0.34	+0.18 (0)
		3.48	0.26	+3.22 (+0.71)
		0.39	0.60	-0.21 (-0.32)
				
High-mountain		0.16	0.55	-0.39 (-0.16)
		0.09	0.30	-0.21 (-0.22)
		1.49	0.63	+0.86 (+1.79)
		0	0.43	-0.43 (-0.42)

temperatures with landscape map. The latter was constructed using the basal areas of landscape groups and the total absorbed parts of these areas. As one can see, the scope of increments of the areas (+ ΔS) in landscape groups was rather great for the region in general: from 5%–10% to 1.5-fold. Reduction of the areas (– ΔS) has a narrower range from 20%–25% to 55%–60%.

By the middle of the 21st century, the areas of semiarid steppes (LG 4) and forest-meadow complexes of river valleys in Ciscaucasia will be substantially extended (by 20%–30%). At the same time, the areas of herb-vermouth-bunch-grass steppes (LG 2) will be reduced. The areas of low-mountain meadow steppes with hornbeam-beech forests (LG 11) will decrease as well due to the expansion of the neighboring oak forests (LG 7). In the middle-mountain layer, broad-leaved forests (LG 6 and 8) will remain in their initial areas.

The areas of upper-mountain pine and birch forests will be significantly extended toward sub-Alps along the Kuban River basin (LG 14 + $\Delta S \approx 0.71 \div 3.22$). At the same time, numerous zones of upper-mountain pine forests (LG 15) scattered over the Central Caucasus will reduce their areas by more than 20%, being replaced by both birch forests of the neighboring LG 14 and the middle-mountain beech forests (LG 8) transgressing here from below.

The active and almost countrywide shift of upper-mountain forests upward along the ridge slopes will considerably reduce the areas of subalpine and even alpine vegetation: by 40% and 20%, respectively. Only the areas of the sub-nival zone will significantly increase (by 85% to 180%). This zone will actively penetrate high mountain deserts and retrieve glaciers, being much less replaced by the alpine zone.

In the Greater Caucasus in general, the upper-mountain landscapes, both forest and meadow steppe, must be characterized by the maximum dynamicity. The thermo- arid trend will manifest itself most dramatically in the middle- and upper-mountain steppified hollows, on the one hand, and at the interface of the sub-nival zone and the zone of high-mountain deserts and glaciers, on the other hand.

7. Conclusion

One should accept certain limitations of predictive ecological models based on the method of actualism. It concerns not only empirical-statistical but also simulation methods of modeling. The prediction may be only for the period of equilibrium or at least stationary processes having the properties of superposition of spatial and temporal coordinates^[63]. The reliability of the models will considerably decrease if the system-forming role of ecological factors cardinaly varies during the forecast period. In this case, the predicted system, being initially linear, will go to the category of nonlinear systems, their distinctive feature being disproportionality of response to a perturbing signal^[64].

However, it may be supposed that these limitations are largely “eliminated” for our models because the models to describe the trajectory of geo(eco)system transformation as a series of successive changes (stages) of its functional states. If we accept, as a first-order approximation, the system relaxation at each stage of this series as equilibrium or stationary non-equilibrium process, following Puzachenko^[65], the process becomes reversible, allowing prediction of the system behavior in terms of basic probability models.

Acknowledgment

This research received no external funding.

Conflict of interest

The author declared no conflict of interest.

References

1. Kotlyakov VM. *Izbrannye sochineniya. Kniga 3. Geografiya v menyayushchemsya mire* (Russian) [Selected works. Book 3. Geography in a changing world]. Moscow: Nauka; 2001.
2. Gerasimov IP. *Ecologicheskie problem v proshloy, nastoyashchey i budushchey geographii Mira* (Russian) [Environmental problems in the past, present and future geography of the world]. Moscow: Nauka; 1985.
3. Sochava VB. *Vvvedenie v uchenie o geosistemah* (Russian) [Introduction into the theory of geosystems]. Novosibirsk: Nauka; 1978.
4. Velichko AA, Borisova OK, Zelikson EM. *Rastitelnost v menyayushchemsya klimate* (Russian) [Vegetation in a changing climate]. *Bulletin of the Academy of Sciences of the USSR* 1991; 3: 82–94.
5. Leemans R. Modelling ecological and agricultural impacts of global change on a global scale. *Journal of Science & Industrial Research* 1992; 51: 709–724.

6. Kobak KI, Kondrasheva NYu, Turchinovich IE. Vliyanie izmeneny klimata na prirodnyuyu zonal'nost' I rkosistemy Rossii (Russian) [Impact of climate change on natural zonality and Russian ecosystems]. In: Izrael YuA (editor). Climate changes and their consequence. St-Petersburg: Nauka; 2002. p. 205–210.
7. Kolomyts EG. Regional'naya model' global'nyh izmeneny prirodnoy sredy (Russian) [Regional model of global environmental changes]. Moscow: Nauka; 2003.
8. Rozenberg GS. Modeli v phytotsenologii (Russian) [Models in Phytocoenology]. Moscow: Nauka; 1984.
9. Kolomyts EG. Boreal'my ekoton i geographicheskaya zonal'nost'. Atlas-Monographiya (Russian) [Boreal ecotone and geographic zonality: Atlas-monograph]. Moscow: Nauka; 2005.
10. Houghton LG, Meira Filho LG, Callander BA, *et al.* (editors). Climate change 1995. The science of climatic change. Cambridge, UK: Cambridge University Press; 1996.
11. Smith TM, Leemance R, Shugart HH. Sensitivity of terrestrial carbon storage to CO₂-induced climate change: Comparison of four scenarios based on general circulation models. *Climatic Change* 1992; 21: 367–384.
12. Komarov A, Chertov O, Zudin S, *et al.* EFIMOD 2—System of simulation models of forest growth and elements cycles in forest ecosystems. *Ecological Modeling* 2003; 170: 373–392.
13. Krambein WC, Graybill FA. An introduction to statistical models in geology. 1st ed. New York: McGraw-Hill Book Company; 1965.
14. Kolomyts EG, Rosenberg GS, Sharaya LS. Metody landshaftnoy ekologii v prognoznnyh otsenkah bioticheskoy regolyatsii uglerodnogo tsikla pri global'nom potepnenii (Russian) [Landscape ecology methods in predictive estimates of the biotic regulation of the carbon cycle during global warming]. *Russian Journal of Ecology* 2009; 6: 1–8.
15. Turner MG, Gardner RH (editors). Quantitative methods in landscape ecology. The analysis and interpretation of landscape heterogeneity. New York, Berlin, Heidelberg: Springer-Verlag; 1990.
16. Saushkin YuG. Geographicheskaya nauka v proshlom, nastouashchem i budushchem (Russian) [Geographical science in the past, present and future]. Moscow: Proshchenie; 1980.
17. Simonov YuG. Osnovnye svoystva ob'ektov geographicheskogo prognozirovaniya i sposoby ih formalizovannogo opisaniya (Russian) [Basic properties of objects of geographical forecasting and methods of their formalized description]. In: Kapitsa AP, Simonov YuG (editors). Problemy regional'nogo geograficheskogo prognoza. Moscow: Nauka; 1982. p. 112–193.
18. Shvidenko AZ. Global'nye izmneneniya I rossiyskaya lesnaya taksatsiya (Russian) [Global changes and Russian forest inventory]. *Forest Inventory and Forest Management* 2012; 47 (1): 52–75.
19. Rozenberg GS, Mozgovoy DP, Gelashvili DB. Ekologiya. Elementy teoreticheskikh konstruktov sovremennoy ekologii (Russian) [Ecology. Elements of theoretical constructs in modern ecology]. Samara: Samarsky Nauchny Tsentr RAN; 1999.
20. Odum EuP. Fundamentals of ecology. 3rd ed. Philadelphia, London, Toronto: W.B. Saunders Company; 1971.
21. Sukachev VN. Izbrannye trudy. Tom 1. Osnovy lesnoy tipologii i biogeostenologii (Russian) [Selected works. Vol. 1. Basics of forest typology and biogeocoenology]. Leningrad: Nauka; 1972.
22. Bazilevich NI, Grebenshchikov OS, Tishkov AA. Geographicheskije zakonomernosti struktury i funkcionirivaniya ekosistem (Russian) [Geographic patterns of the structure and functioning of ecosystems]. Moscow: Nauka; 1986.
23. Armand AD, Targul'an VO. Nekorye printsipial'nye ogranocheniy experimenta i modelirovaniya v geographii (Russian) [Some fundamental limitations of experiment and modeling in geography]. *Izvestiya RAN (Akad. Nauk SSSR). Seriya Geograficheskaya* 1974; 4: 129–138.
24. Kolomyts EG. Lokal'nye mekhanizmy global'nyh izmeneny prirodnyh ekosistem (Russian) [Local mechanisms of global changes in natural ecosystems]. Moscow: Nauka; 2008.
25. Albritton DL, Barker T, Bashmakov I, *et al.* Changing of the climate. 2001. In: Whotson RT (editor). Synthesis report MGEIK. Geneva: World Meteorological Organization; 2003.
26. Dokuchaev VV. Uchenie o prirodnyh zonah. Gorizonta'lnae b vertikal'nye pochvennye zony (Russian) [To the doctrine of natural zones. Horizontal and vertical soil zones]. St.-Petersburg: Printing House of St.-Petersburg City Administration; 1899.
27. Berg LS. Gtographicheskije zony Sovetskogo Soyuz (Russian) [Geographic zones of the Soviet Union]. Moscow: Geographgiz; 1947.
28. Grigor'ev AA. Zakonomernosti stroeniya I razvitiya geographicheskoy sredy (Russian) [Regularities of the structure and development of the geographic environment]. Moscow: Mysl'; 1966.
29. Budyko MI. Global'naya ekologiya (Russian) [Global ecology]. Moscow: Mysl'; 1977.
30. Mil'kov PhN. Phizicheskaya geographiya: Uchenie o landshafte i geographicheskaya zonal'nost' (Russian) [Physical geography: The doctrine of the landscape and the geographic zonality]. Voronezh: Voronezh Publishing House University; 1986.
31. Gribova SA, Isachenko TI, Lavrenko EM. Rastitel'nost' Evropeyskoy chasti SSSR (Russian) [Vegetation of the European part of the USSR]. Leningrad: Nauka; 1980.
32. Köppen V. Osnovy klimatologii (Klimaty Zemnogo Shara) (Russian) [Fundamentals of climatology (climates of the globe)]. Moscow: Uchpedgiz; 1938.
33. Vysotsky GN. Izbrannye Trudy (Russian) [Selected works]. Moscow: Selkhozgiz; 1960.
34. Armand DL. Nauka o landshafte (Russian) [Science about landscape]. Moscow: Mysl'; 1975.
35. Isachenko AG. Landshafty SSSR (Russian) [Landscapes of the USSR]. Leningrad: Publishing House of Leningrad State University; 1985.
36. Timofeev-Resovsky NV, Tyuryukanov AN. Ob elementarnykh biohorologicheskikh podrazdeleniyah biosfery (Russian) [On elementary bichorologic subdivisions of the biosphere]. *Byulleten' Moskovskogo Obshchestva Ispytatelei Prirody Otdel Biologicheskii* 1966; LXXI(1): 123–132.
37. Andreev VL. Klassifikatsionnye postroeniya v ekologii i sistematike (Russian) [Classification constructs in ecology and systematics]. Moscow: Nauka; 1980.
38. Syomkin BI. Deskriptivnye mnozhestvas i ih prilozheniya (Russian) [Descriptive sets and their applications]. In: Syomkin BI (editor). Research of systems. 1. Analysis of complex systems. Vladivostok: Pacific. Institute of Geography. Far East Scientific Center of the Academy of Sciences of the USSR; 1973. p. 83–94.
39. Harbaugh JW, Bonham-Carter G. Computer simulation in geology. New York, London, Sydney, Toronto: Wiley-Interscience; 1970.
40. Gordon C, Cooper C, Senior CA, *et al.* The simulation of

- SST, sea ice extents and ocean heat transport in a version of the Hadley Centre coupled model without flux adjustments. *Climate Dynamics* 2000; 16: 147–168. doi: 10.1007/s003820050010.
41. Pope VD, Gallani ML, Rowntree PR, Stratton RA. The impact of new physical parametrizations in Hadley Centre climate model: HadCM3. *Climate Dynamics* 2000; 16: 123–146. doi: 10.1007/s003820050009.
 42. Schmidt GA, Ruedy R, Hansen JE, *et al.* Present day atmospheric simulations using GISS Model E: Comparison to in-situ, satellite and reanalysis data. *Journal Climate* 2006; 19: 153–192.
 43. Hansen J, Sato M, Ruedy R, *et al.* Dangerous human-made interference with climate: A GISS model E study. *Climate Dynamics* 2007; 7: 2287–2312. doi: 10.5194/acp-7-2287-2007.
 44. Menzhulin GV, Savvateev SP. Mirovaya prodovol'stvennaya problema I sovremennoe global'noe poteplenie (Russian) [World food program and contemporary global warming]. In: Budyko MI (editor). *Izmeneniya klimata i ego posledstviya*. St-Petersburg: Nauka; 2002. p. 122–151.
 45. Kolomyts EG, Sharaya LS. Vliyanie global'nogo potepleniya na landshaftnyu strukturu Severnogo Kavkaza (Russian) [The impact of global warming on the landscape structure of the North Caucasus]. *Izvestiya RAN. Seriya Geograficheskaya* 2012; 4: 52–68.
 46. Kustler G. ABC of information theory. In: Yockey HP (editor). *Information theory in biology*. London, New York, Los Angeles: Pergamon Press; 1957. p. 5–48.
 47. Volobuev VR. Vvedenie v energetiku pochvoobrazovaniya (Russian) [Introduction to the energetics of soil formation]. Moscow: Nauka; 1974.
 48. Gerasimov IP, Velichko AA (editors). *Paleogeografiya Evropy za poslednie sto tysyach let (Atlas-mionografiya)* (Russian) [Paleogeography of Europe for the last hundred thousand years (Atlas-monography)]. Moscow: Nauka; 1982.
 49. Velichko AA, Grichuk VP, Gurtovaya EE, Zelikson EM. Paleoklimat territorii SSSR v optimum poslednego (mikulinskogo) mezhlenikov'ya (Russian) [Paleoclimate of the territory of the USSR at the optimum of the last (Mikulino) interglacial]. *Izvestiya RAN (Akad. Nauk SSSR). Seriya Geograficheskaya* 1983; 6: 30–45.
 50. Velichko AA, Klimanov VA. Klimaticheskie usloviya Severnogo polushariya 5–6 tysyach let nazad (Russian) [Climatic conditions of the Northern Hemisphere 5–6 thousand years ago]. *Izvestiya RAN (Akad. Nauk SSSR). Seriya Geograficheskaya* 1990; 5: 38–52.
 51. Neishtadt MI. Regional'nye zakonomernosti istorii phytotsenozov SSSR v golotsene po paleogeograficheskim dannym (Russian) [Regional patterns of the history of phytocenoses of the USSR in the Holocene according to palynological data]. In: Gerasimov IP (editor). *History of biogeocenoses of the USSR in the Holocene*. Moscow: Nauka; 1976. p. 79–91.
 52. Beruchashvili NL, Arutyunov SR, Tediashvili AG. Landshaftnaya karta Kavkaza. M-b: 1:1000 000 (Russian) [Landscape Map of the Caucasus. Sc. 1:1000 000]. Tbilisi: Izdatel'stvo Tbilisskogo un-ta; 1979.
 53. Izrael YuA (editor). *Sostoyanie I kompleksny monitoring prirodnoy sredy i klimata. Predely izmeneny* (Russian) [Condition and comprehensive monitoring of the natural environment and climate. Limits of change]. Moscow: Nauka; 2001.
 54. Volobuev VR. *Ekologiya pochv (oserkii)* (Russian) [Soil ecology (essays)]. Baku: Publishing House of AN Azerb. SSR; 1963.
 55. Emanuel WR, Shugart HH, Stevenson MR. Climatic changes and the boreal-scale distribution of terrestrial ecosystem complexes. *Climatic Change* 1985; 7: 29–43. doi: 10.1007/BF00139439
 56. Holten JI, Paulsen G, Oechel WC (editors). *Impacts of climatic change on natural ecosystems (with emphasis on boreal and arctic/alpine areas)*. Trondheim: NINA and DN; 1993.
 57. Shary PA. *Analytical GIS Eco* [Internet]. GIS Eco; 2001. Available from: <http://www.giseco.info>.
 58. MacMillan RA, Torregrosa A, Moon D, *et al.* Automated predictive mapping of ecological entities. In: Hengl T, Reuter HT (editors). *Geomorphometry: Concepts, software, applications. Developments in soil science*. Amsterdam, The Netherlands: Elsevier; 2009. p. 551–578. doi: 10.1016/S0166-2481(08)00024-X.
 59. Shary PA. Models of topography. In: Zhou Q, Lees B, Tang G (editors). *Advances in digital Terrain analysis. Lecture notes in geoinformation and cartography*. Berlin: Springer-Verlag; 2008. p. 29–57.
 60. Sharaya LS. Predskazatel'noe kartirovanie lesnykh ekosistem v geoekologii (Russian) [Predictive mapping of forest ecosystems in geoecology]. *Povolzhskiy Ecological Journal* 2009; 3: 249–257.
 61. Pike RJ, Evans IS, Hengl T. Geomorphometry: A brief guide. In: Hengl T, Reuter HI (editors). *Geomorphometry: Concepts, software, applications. Developments in soil science*. Amsterdam, The Netherlands: Elsevier; 2009. p. 3–30. doi: 10.1016/S0166-2481(08)00001-9.
 62. Shary PA, Sharaya LS, Mitusov AV. Fundamental quantitative methods of and surface analysis. *Geoderma* 2002; 107(1–2): 1–32. doi: 10.1016/S0016-7061(01)00136-7.
 63. Puzachenko YuG. *Metodologicheskie osnovy geographicheskogo prognoza i ohrany sredy* (Russian) [Methodological foundations of geographical forecasting and environmental protection]. Moscow: URAO Publishing House; 1998.
 64. Zeydis IM, Kruzhalin VI, Simonov YuG, *et al.* *Obshchie svoystva dinamiki geosistem* (Russian) [General properties of the dynamics of geosystems]. *Vestnik MGU. Seriya 5. Geografiya* 2001; (4): 3–8.
 65. Puzachenko YuG. Invariantnost' geosistem i ih komponentov (Russian) [Invariance of geosystems and their components]. In: Armand AD, Dolgushin Iyu (editors). *Stability of geosystems*. Moscow: Nauka; 1983. p. 32–41.